Project B.10 – Study of Flammability of Materials

Flammability Testing of Automotive Heating Ventilation and Air Conditioning Modules Made from Polymers Containing Flame Retardant Chemicals

Jeffrey Santrock
General Motors Corporation

Archibald Tewarson and Peter K. S. Wu
Factory Mutual Research Corporation

Abstract

Flammability tests were conducted on three automotive Heating Ventilation and Air Conditioning (HVAC) modules. These tests were conducted at the Factory Mutual Global Test Center in West Glocester, Rhode Island. One control HVAC module was used in these tests and was made of plastic materials that did not contain flame retardant chemicals. Two experimental HVAC modules were used in these tests and were made of plastic materials that contained flame retardant chemicals. The HVAC modules were placed above a heptane pool fire. Products from the burning heptane and HVAC modules were drawn into the Fire Products Collector at the test facility. The mass loss rates of the control and experimental HVAC modules were similar. The energy yields from the experimental HVAC modules were approximately 50% of the energy yield from the control HVAC module. The poly(propylene) parts in the control HVAC module contained calcium carbonate. Carbon dioxide produced from the calcium carbonate interfered with accurate measurement of the carbon dioxide produced from combustion of the plastic materials in the control HVAC module. Thus a more accurate estimation of the heat release rate from the control HVAC module was impossible. The yields of carbon monoxide from the two HVAC modules containing flame retardant chemicals were 897 and 751% of the yield of carbon monoxide from the control HVAC module. The yields of hydrocarbon from the two HVAC modules containing flame retardant chemicals were 5,567 and 4,867% of the yield of hydrocarbons from the control HVAC module. The yields of smoke from the two HVAC modules containing flame retardant chemicals were 4,725 and 3,875% of the yield of smoke from the control HVAC module, which is consistent with visual observations made during these tests that the experimental HVAC modules produced substantially more smoke than the control HVAC module.

Introduction

The tests described in this report were conducted by General Motors (GM) and by Factory Mutual Research Corporation under contract by GM pursuant to an agreement between GM and the United States Department of Transportation. This report describes flammability tests that were conducted on one control and two experimental automotive Heating Ventilation and Air Conditioning (HVAC) modules. Plastic materials in the control HVAC module did not contain flame retardant chemicals. The poly(propylene) and polyester materials in the two experimental HVAC modules contained flame retardant chemicals.

Flammability tests on each of the three HVAC modules were conducted to determine rates of production of heat energy and fire products.

Experimental

HVAC Modules. The HVAC modules used in this test were for a 1999 Chevrolet Camaro. Table 1 lists the masses of selected components in this HVAC module assembly and the materials used in these components. The components of the HVAC module assembly listed in Table 1 include the Air Inlet and Outlet Housing, Auxiliary A/C Evaporator and Blower Upper Case, Auxiliary A/C Evaporator and Blower Lower Cases, Heater Front Case, Heater Rear Case, Heater Case, Air Distribution Case, A/C Evaporator Core, Heater Core, Mode Valve, and Blower Motor.

None of the materials in the control HVAC module used in these tests contained flame retardant chemicals. The poly(propylene) and polyester parts in the two experimental HVAC modules used in these tests contained flame retardant chemicals. The Air Inlet and Outlet Housing, Auxiliary A/C Evaporator and Blower Upper Case, Heater Front Case, Heater Rear Case, Heater Case, and Air Distribution Case were molded from poly(propylene) resin containing decabromodiphenyleneoxide, antimony trioxide, and zinc-based flame retardant chemicals (Table 2). Auxiliary A/C Evaporator and Blower Lower Cases containing two different formulations of flame retardant chemicals were molded from polyester resins containing antimony trioxide and alumina silicate or alumina hydrate flame retardant chemicals (Table 2). The experimental HVAC modules were designated FR1 and FR2 to indicate the different flame retardant chemical formulations in the Auxiliary A/C Evaporator and Blower Lower Cases. The poly(propylene) components in FR1 and FR2 were the same.

Table 1

Material and Mass of HVAC Parts

Component	Material[1]	Mass (kg)
Air Inlet and Outlet Housing	PP	0.27
Auxiliary A/C Evaporator and Blower Upper Case	PP	0.55
Auxiliary A/C Evaporator and Blower Lower Case	PE	2.03
Heater Front Case	PP	0.58
Heater Rear Case	PP	0.31
Heater Case	PP	0.24
Air Distribution Case	PP	0.58
A/C Evaporator Core	AL	1.86
Heater Core	AL	0.64
Mode Valve	ST	0.26
Blower Motor	ST / FE / CU	1.31
HVAC Module	n/a	9.70

[1] AL = aluminum; CU = copper; FE = iron; PE = polyester; PP = poly(propylene); ST = steel.

Table 2

Additives in the Poly(propylene) and Poly(ester) Parts of the HVAC Modules

	poly(propylene)	polyester
Control	$Ca(CO_3)$	glass fiber clay cissel
FR1	decabromodiphenyleneoxide SbO_3 Zn-compounds	glass fiber SbO_3 $Al_2O_3 \bullet (SiO_2)$
FR2	decabromodiphenyleneoxide SbO_3 Zn-compounds	glass fiber $Al_2O_3 \bullet H_2O$

Fire Products Collector. Flammability tests were conducted at the Factory Mutual Global Test Center in West Glocester, Rhode Island. A fire products collector [1] was used to measure heat and combustion gases generated by the burning HVAC modules during these tests (Fig. 1).

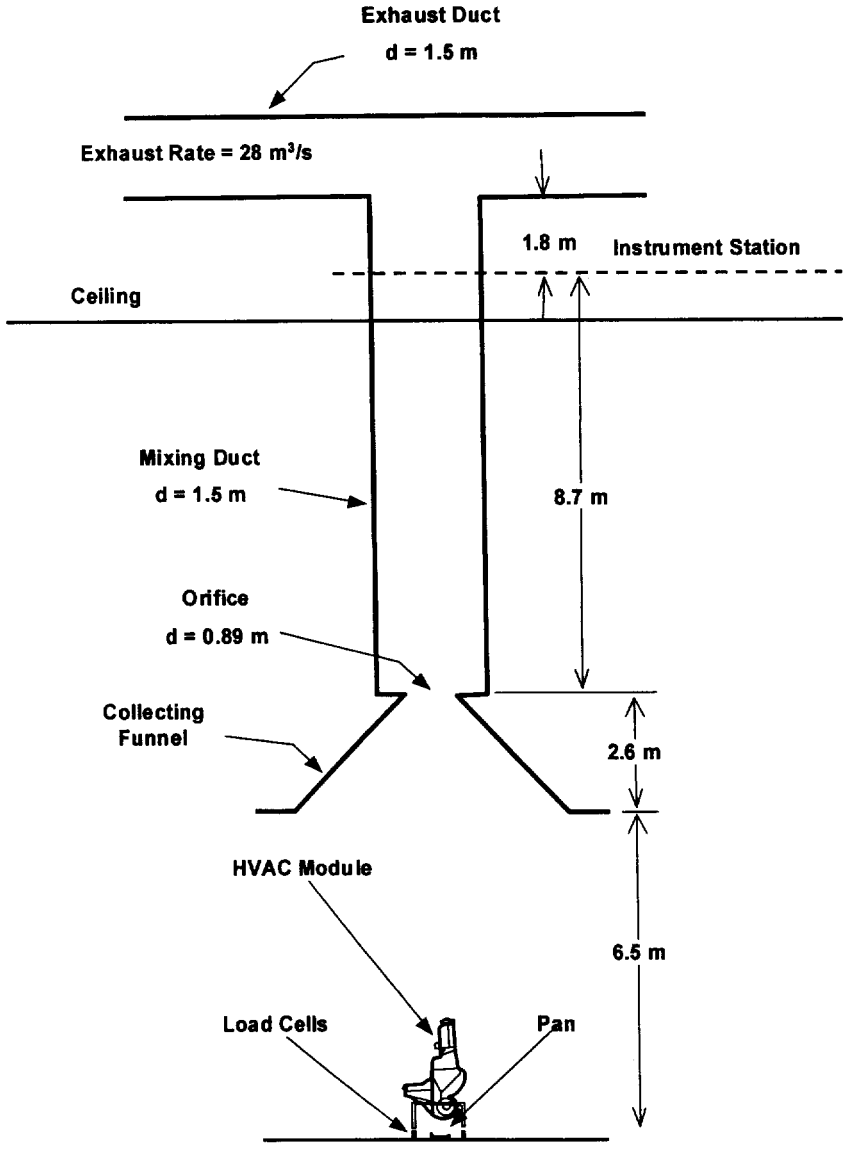

Figure 1. Diagram of an HVAC module under the fire products collector at the Factory Mutual Test Center.

The fire products collector consisted of a collection funnel (diameter = 6.1 m), an orifice plate (hole = 0.9 m), and a vertical stainless steel sampling duct (diameter = 1.5 m). The sampling duct was connected to the air pollution control system of the Test Center. The blower of the air pollution control system induces gas flow through the sampling duct. Air enters the sampling duct via the orifice plate. The temperature, linear velocity, optical transmission, and chemical

composition of the entrained gas were measured in the center of the sampling duct 8.66 m (5.7 duct diameters) downstream from the orifice plate, ensuring a flat velocity profile at the sampling location. The data acquisition system consisted of a Hewlett Packard 2313B analog-to-digital conversion sub-system interfaced to a Hewlett Packard 1000 computer.

Gas temperature in the sampling duct was measured with two Type-K thermocouples (30 gage) with exposed bead-type junctions. The thermocouple leads were housed in stainless steel tubes (o.d. = 6.4 mm). Ambient air temperature in the facility was measured by five Type-K thermocouples attached to the external surface of the duct at 2.44, 5.49, 9.14, 12.8, and 15.9 m above the floor. These thermocouples were shielded from radiation from the fire.

The linear velocity of the gas entrained in the sampling duct was measured with a Pitot ring consisting of four Pitot tubes. A static pressure tap was mounted on the inside wall of the sampling duct. The pressure difference between the Pitot ring and the static wall tap was measured with an electronic manometer (Barocel Model 1173, CGS Scientific Corporation).

The particulate concentration in the entrained air was determined from the optical transmission across the duct measured at 0.4579 μm (blue), 0.6328 μm (red), and 1.06 μm (infrared). The optical path length across the duct was 1.524 m. Gas was withdrawn from the sampling duct through a stainless steel tube (o.d. = 3.9 mm) at a flow rate of 0.17×10^{-3} m^3/s for chemical analysis. The gas flowed through a particulate filter, a water condenser, and a drying agent before entering the analyzers. Carbon dioxide (CO_2) and carbon monoxide (CO) were measured with two non-disperse infrared analyzers (Beckman Model 864 Infrared Analyzers). Oxygen (O_2) was measured with a paramagnetic oxygen analyzer (Beckman Model 755 Paramagnetic Oxygen Analyzer). The concentration of the mixture of gaseous hydrocarbons (total hydrocarbons) was measured with a flame ionization analyzer (Beckman Model 400 Flame Ionization Analyzer).

The rate of product release G_j was calculated using the following relationship:

$$G_j = \left(\frac{dR_j}{dt} \right) = f_j \left(\frac{dV}{dt} \right) \rho_j = f_j \left(\frac{dW}{dt} \right) \left(\frac{\rho_j}{\rho_g} \right) \qquad (1)$$

where $d(R_j)/dt$ is the mass release rate of product j in kg/s; f_j is the volume fraction of product j; dV/dt is the total volume flow rate of the gas entrained in the sampling duct in m^3/s; dW/dt is the total mass flow rate of the gas entrained in the sampling duct in kg/s; ρ_j is the density of product j in g/m^3; and ρ_g is the density of the gas entrained in the concentration measurements in g/m^3.

The rate of oxygen consumption was calculated using equation (1), where the volume fraction of oxygen consumed was substituted for f_j.

The volume fraction of smoke particulate (f_S) was calculated from the following relationship:

$$f_s = \frac{D\lambda \times 10^{-6}}{\Omega} \tag{2}$$

where f_s is the volume fraction of smoke, λ is the wavelength of the light source, Ω is the extinction coefficient of particulate (a value of 7.0 was used in these calculations), and D is the optical density at each of the three wavelengths at which measurements were made:

$$D = \frac{\ln\left(I_0/I\right)}{L} \tag{3}$$

where I_0 is the intensity of light transmitted through clean air, I is the intensity of light transmitted through air containing smoke particulate, and L is the optical path length, which was equal to 1.524 m. A value of 1.1×10^6 g/m^3 was used for the density of smoke particulate (ρ_j) in equation (1).

The convective heat release rate (Q_{CONV}) was calculated using the following relationship:

$$Q_{CONV} = \left(\frac{dE_{CONV}}{dt}\right) = \left(\frac{dW}{dt}\right) \times c_p \times \left(T_g - T_a\right) \tag{4}$$

dW/dt is the mass flow rate of the gas entrained in the sampling duct in kg/s; c_p is the heat capacity of the gas entrained in the sampling duct at the gas temperature in kJ/(kg×K); T_g is the temperature of the gas entrained in the sampling duct in K; and T_a is the ambient air temperature in K.

The chemical heat release rate was calculated from the release rates of carbon dioxide and carbon monoxide ($Q_{CHEM}^{CO_2}$) as follows:

$$Q_{CHEM}^{CO_2} = \left(\frac{dE_{CHEM}}{dt}\right) = \Delta H_{CO_2}^{*} \times \left(\frac{dR_{CO_2}}{dt}\right) + \Delta H_{CO}^{*} \times \left(\frac{dR_{CO}}{dt}\right) \tag{5}$$

ΔH^*_{CO2} is the net heat of complete combustion per unit mass of carbon dioxide released by the fire in kJ/g, ΔH^*_{CO} is the net heat of complete combustion per unit mass of carbon monoxide released by the fire in kJ/g; dR_{CO2}/dt is the mass release rate of carbon dioxide in kg/s; and dR_{CO}/dt is the mass release rate of carbon monoxide in kg/s. Values of ΔH^*_{CO2} and ΔH^*_{CO} were obtained from the literature [2].

The chemical heat release rate also was calculated from the oxygen consumption rate ($Q^{O_2}_{CHEM}$) as follows:

$$Q^{O_2}_{CHEM} = \left(\frac{dE_{CHEM}}{dt}\right) = \Delta H^*_{O_2}\left(\frac{dC_{O_2}}{dt}\right) \qquad (6)$$

where $d(E_{CHEM})/dt$ is the chemical heat release rate in kW; ΔH^*_{O2} is the net heat of complete combustion per unit mass of O_2 consumed in kJ/g; and $d(C_{O2})/dt$ is the consumption rate of oxygen in kg/s. The value for ΔH^*_{O2} was obtained from the literature [2].

Mass loss from the burning HVAC modules was measured with a load cell weigh-module system (KIS Series, BLH Electronics, Inc.) on a support stand.

Flammability Tests. Each HVAC module was mounted to a stand so that the module was oriented vertically. The base of the stand was 6.5 m below the opening of the collection duct of the Fire Products Collector. The ignition source for the HVAC modules was a pool of heptane (1450 mL) contained in a metal pan (9 in. x 9 in.) located below the center of the HVAC module. The heptane was ignited using a propane torch. to start each test.

Results

Approximately 58% (wt/wt) of the HVAC modules used in these tests consisted of organic polymers (plastics), while metal comprised the remaining and 42% (wt/wt) of the HVAC modules was metal (Table 1). The poly(propylene) and polyester parts containing flame retardant chemical additives constituted approximately 81% (wt/wt) of the combustible materials in the two experimental HVAC modules.

The HVAC modules ignited between 30 and 60 seconds after ignition of the heptane. The heptane ignition source burned for approximately 11 minutes in these tests, and the HVAC modules were allowed to burn for an additional 4 to 5 minutes.

Data recorded from the fire products collector included ambient air temperature, barometric pressure, gas temperature, gas flow rate, carbon dioxide concentration (C_{CO2}), carbon monoxide concentration (C_{CO}), total hydrocarbons concentration (C_{HC}), oxygen concentration (C_{O2}), turbidity at λ = 0.4679 μm, turbidity at λ = 0.6318 μm, turbidity at 1.06 μm. Data from the load cells on the HVAC module test stand also was recorded.

Data from the fire products collector acquired with only the heptane ignition source burning (no HVAC module) is shown in Appendix A. Data from the fire products collector acquired during the test of the control HVAC module is shown in Appendix B. Data from the fire products collector acquired during the test of the FR1 HVAC module is shown in Appendix C. Data from the fire products collector acquired during the test of the FR2 HVAC module is shown in Appendix D.

Plots of the carbon dioxide release rates (G_{CO2}), the carbon monoxide release rates (G_{CO}), the hydrocarbon release rates (G_{HC}), and the oxygen consumption rates (G_{O2}) for the control HVAC module, the two experimental HVAC modules, and the heptane ignition source are shown in Figures 2 through 5. G_{CO2}, G_{CO}, G_{HC}, and C_{O2} were determined from the C_{CO2}, C_{CO}, C_{HC}, and C_{O2} data in Appendices A through D using equation 1.

Plots of the smoke release rate (G_{SMOKE}) for the control HVAC module, the two experimental HVAC modules, and the heptane ignition source are shown in Figure 6. C_{SMOKE} was determined from the turbidity at λ = 0.6318 μm data in Appendices A through D using equations 2 and 3. G_{SMOKE} was determined from C_{SMOKE} using equation 1.

Plots of the convective heat release rate (Q_{CONV}) for the control HVAC module, the two experimental HVAC modules, and the heptane ignition source are shown in Figure 7. Q_{CONV} was determined from the ambient air temperature and the gas temperature in the fire products collector using equation 4.

Plots of the chemical heat release rates for the control HVAC module, the two experimental HVAC modules, and the heptane ignition source are shown in Figures 8 and 9. Figure 8 shows $Q_{CHEM}^{CO_2}$ determined from G_{CO2} and G_{CO} using equation 5. Figure 9 shows $Q_{CHEM}^{O_2}$ determined from G_{O2} using equation 6.

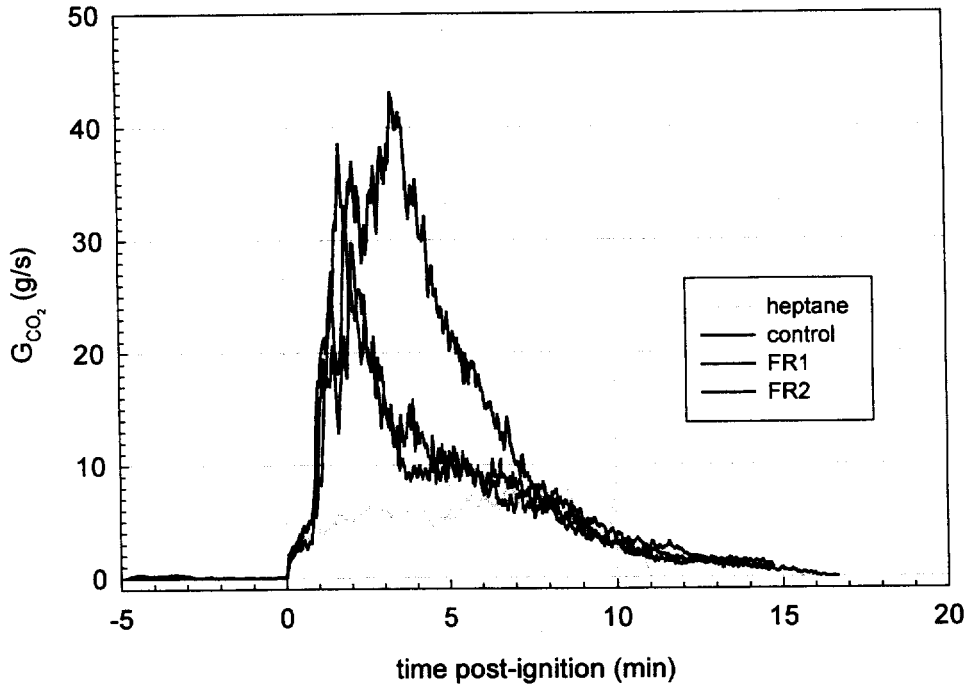

Figure 2. Carbon dioxide release rate (G_{CO2}) curves for the control + heptane ignition source, the FR1 HVAC module + heptane ignition source, and the FR2 HVAC module + heptane ignition source. The carbon dioxide release rate curve for the heptane ignition source is shown for reference.

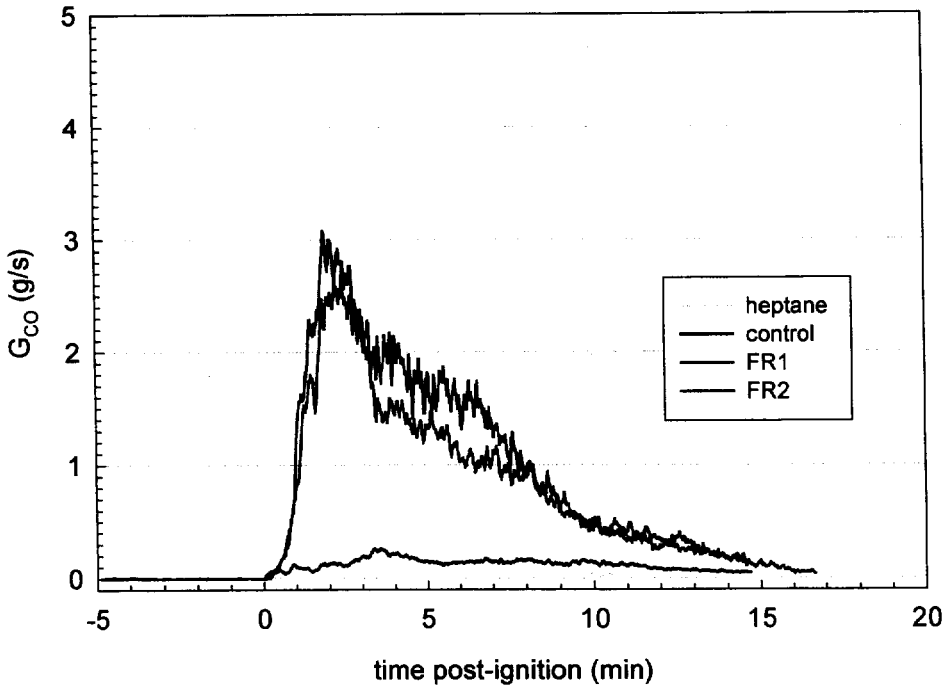

Figure 3. Carbon monoxide release rate (G_{CO}) curves for the control + heptane ignition source, the FR1 HVAC module + heptane ignition source, and the FR2 HVAC module + heptane ignition source. The carbon dioxide release rate curve for the heptane ignition source is shown for reference.

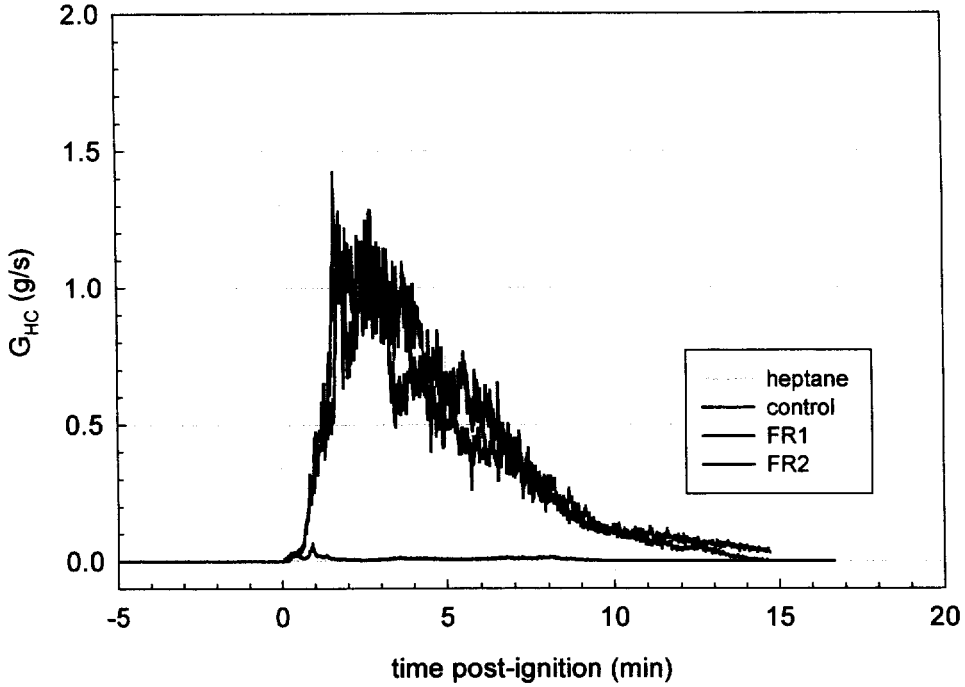

Figure 4. Hydrocarbon release rate (G_{HC}) curves for the control + heptane ignition source, the FR1 HVAC module + heptane ignition source, and the FR2 HVAC module + heptane ignition source. The hydrocarbon release rate curve for the heptane ignition source is shown for reference.

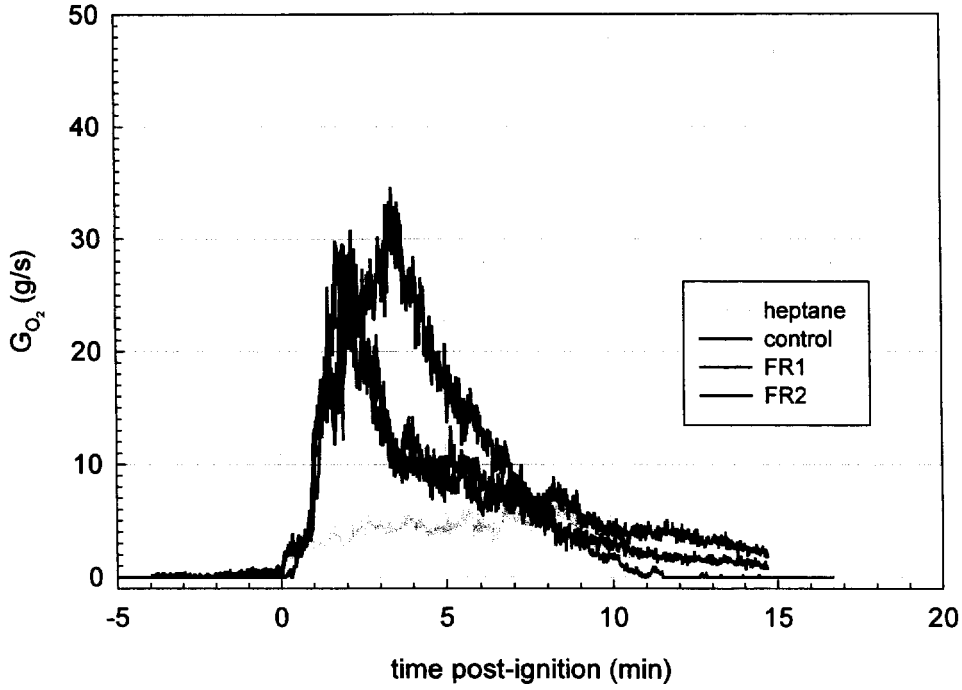

Figure 5. Oxygen consumption rate (G_{O2}) curves for the control + heptane ignition source, the FR1 HVAC module + heptane ignition source, and the FR2 HVAC module + heptane ignition source. The oxygen consumption rate curve for the heptane ignition source is shown for reference.

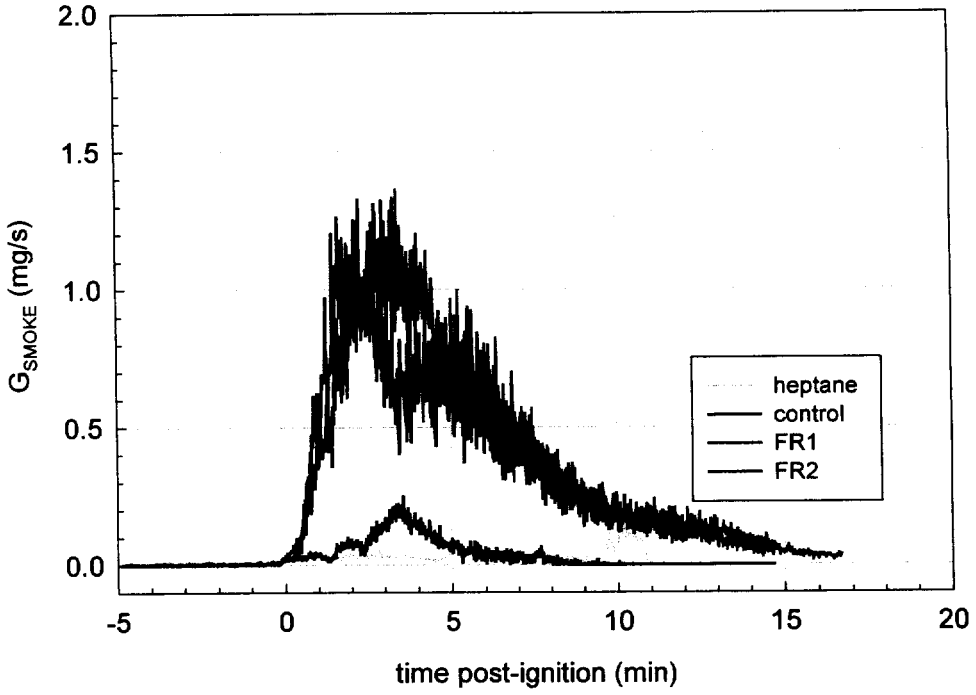

Figure 6. Smoke release rate (G_{SMOKE}) curves for the control + heptane ignition source, the FR1 HVAC module + heptane ignition source, and the FR2 HVAC module + heptane ignition source. The smoke release rate curve for the heptane ignition source is shown for reference.

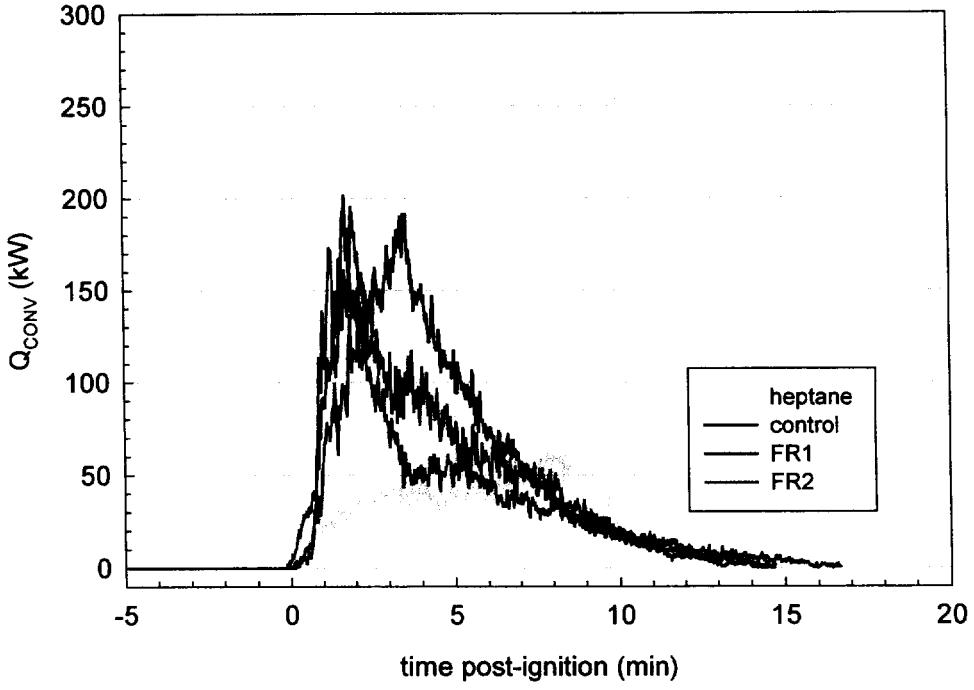

Figure 7. Convective heat release rate (Q_{CONV}) curves for the control + heptane ignition source, the FR1 HVAC module + heptane ignition source, and the FR2 HVAC module + heptane ignition source. The convective heat release rate curve for the heptane ignition source is shown for reference

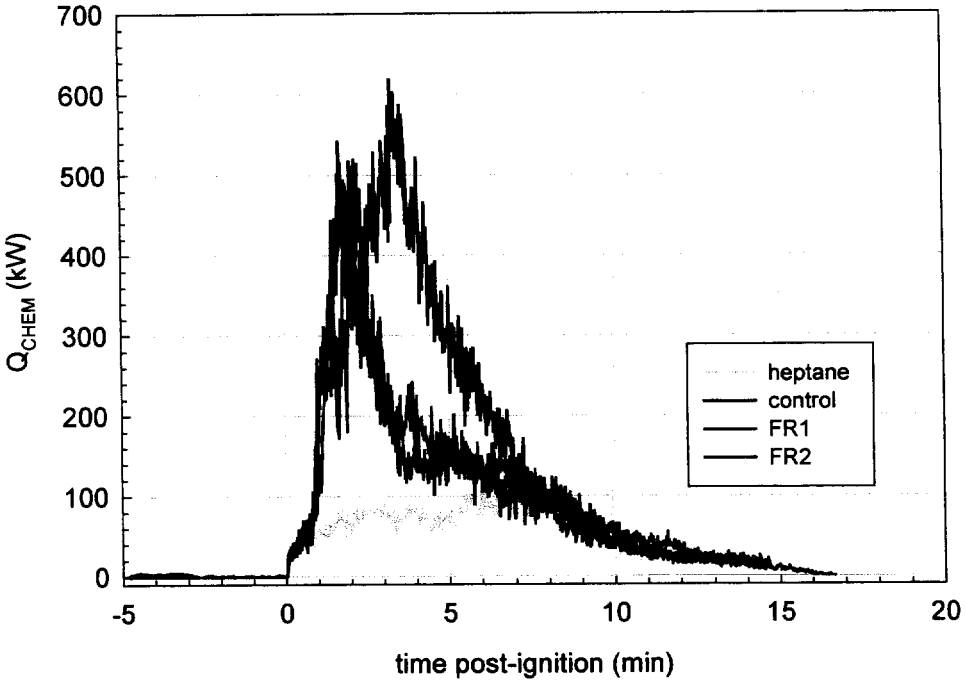

Figure 8. Chemical heat release rate ($Q_{CHEM}^{CO_2}$) curves calculated from G_{CO2} and G_{CO} for the control + heptane ignition source, the FR1 HVAC module + heptane ignition source, and the FR2 HVAC module + heptane ignition source. The chemical heat release rate curve for the heptane ignition source is shown for reference.

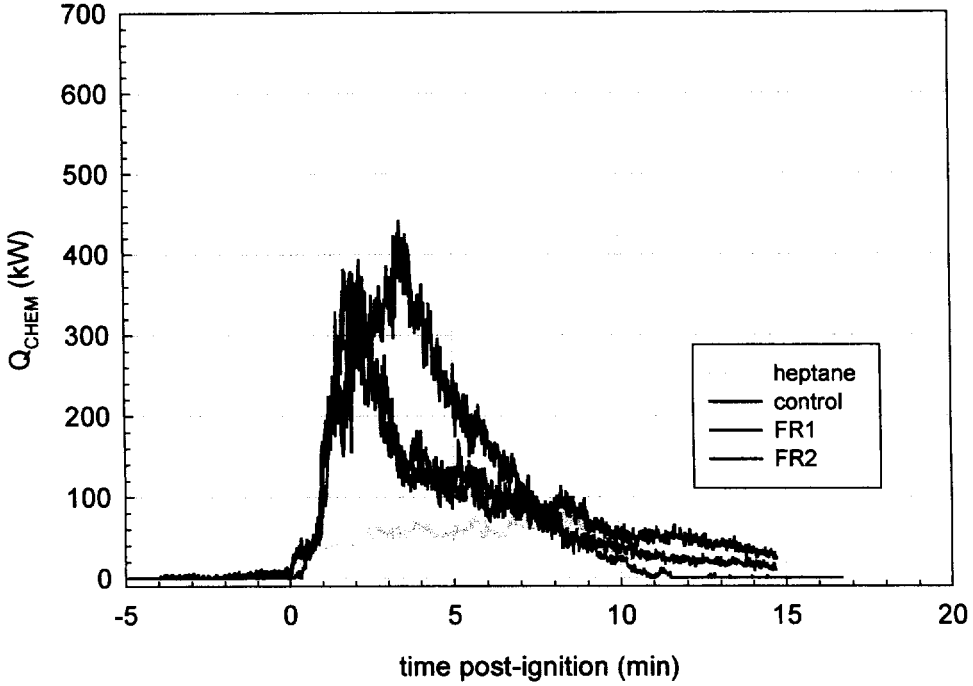

Figure 9. Chemical heat release rate ($Q_{CHEM}^{O_2}$) curves calculated from G_{CO2} for the control + heptane ignition source, the FR1 HVAC module + heptane ignition source, and the FR2 HVAC module + heptane ignition source. The chemical heat release rate curve for the heptane ignition source is shown for reference.

The mass loss, energy yield, carbon dioxide yield, carbon monoxide yield, total hydrocarbon yield, smoke yield, and oxygen consumption for the control HVAC module and the two experimental HVAC modules are shown in Table 3. The mass loss was determined from the mass loss curves in Appendices A through D. The energy yields in Table 3 for the control and experimental HVAC modules were determined by integrating $Q_{CHEM}^{CO_2} \cdot dt$ and $Q_{CHEM}^{O_2} \cdot dt$, and subtracting the values obtained by integrating the curve for the heptane igniter (Fig.'s 8 and 9). The carbon dioxide yield, carbon monoxide yield, total hydrocarbon yield, smoke yield and oxygen consumption were determined by integrating $G_{CO_2} \cdot dt$, $G_{CO} \cdot dt$, $G_{HC} \cdot dt$, $G_{SMOKE} \cdot dt$ and $G_{O_2} \cdot dt$ and subtracting the values obtained by integrating curves for the heptane igniter (Fig.'s 2 through 6).

Table 3

Summary of Mass Loss, Energy and Chemical Product Yields for the Control and Experimental HVAC Modules

HVAC Module/ Fire Test Data		Control	FR1	FR2
Mass Loss (g)		4296	4303	4165
Energy Yield (MJ)	$Q_{CHEM}^{CO_2}$	105	54	48
	$Q_{CHEM}^{O_2}$	80	34	53
Carbon Dioxide Yield (g)		7660	3324	2907
Carbon Monoxide Yield (g)		107	960	804
Total Hydrocarbon Yield (g)		6	334	292
Smoke Yield (mg)		8	378	310
Oxygen Consumed (g)		6128	2807	4118

The energy yields from FR1 and FR2 derived from $Q_{CHEM}^{CO_2}$ were 51 and 46 % of the energy yield from the control. The energy yields from FR1 and FR2 derived from $Q_{CHEM}^{O_2}$ were 42 and 66% of the energy yield from the control. For pure polymers, $Q_{CHEM}^{CO_2}$ is generally considered to be more reliable than $Q_{CHEM}^{O_2}$ because the precision in measuring changes in C_{CO2} resulting from a fire is greater than the precision in measuring changes in C_{O2}. The reason for the greater precision in the measurement of C_{CO2} compared to C_{O2} is that the concentration of CO_2 in air is between 350 and 400 ppm, while the concentration of O_2 in air is approximately 21% (210,000 ppm). Although the amount (number of molecules) of O_2 consumed when an organic polymer burns is greater

than the amount of CO_2 produced, the relative increase in the concentration of CO_2 in air is considerably greater than the relative decrease in the concentration of O_2. For example, the plot of C_{CO2} dioxide measured during the test of the control HVAC module (Plot B1, **APPENDIX B**) shows that the maximum concentration of carbon was approximately 1700 ppm, a 480% increase in the CO_2 concentration in ambient air. The plot of C_{O2} measured during the test of the control HVAC module (Plot B4, **APPENDIX B**) was approximately 20.73%, a 1% decrease in the O_2 concentration in ambient air.

Calcium carbonate ($Ca(CO_3)$) in the poly(propylene) parts in the control HVAC module (Table 2) may have resulted in a systematic error in estimating the heat release rate form $Q_{CHEM}^{CO_2}$. When heated in a fire, $Ca(CO_3)$ decomposes to CO_2 and CaO. Carbon dioxide produced from the $Ca(CO_3)$ in the polypropylene during the test of the control HVAC module would have resulting in a higher CO_2 concentration in the air flowing into the fire products collector than if pure poly(propylene) were burning, which in turn would have resulted in a systematic overestimation of actual heat release rate from $Q_{CHEM}^{CO_2}$.

The yield of incomplete oxidation products, which includes carbon monoxide, total hydrocarbons, and smoke, was greater from FR1 and FR2 than from the control HVAC module. The yields of carbon monoxide from FR1 and FR2 were 897 and 751% of the yield of carbon monoxide from the control HVAC module (Table 3). The yields of total hydrocarbon from FR1 and FR2 were 5,567 and 4,867% of the yield of total hydrocarbons from the control HVAC module (Table 3). The yields of smoke from FR1 and FR2 were 4,725 and 3,875% of the yield of smoke from the control HVAC module (Table 3), which is consistent with visual observations made during these tests that FR1 and FR2 produced substantially more smoke than the control HVAC module.

DISCUSSION

The effect of the chemical flame retardant additives in the poly(propylene) and polyester parts in the experimental HVAC modules appears to have resulted in a decrease in the efficiency of combustion in the gas phase. As indicated by the similar mass losses of the control and two experimental HVAC modules, these chemical additives did not produce measurable differences in the mass loss characteristics of the experimental HVAC modules when compared to the control HVAC module. Chemical analysis indicated that thermal decomposition products of the poly(propylene) and polyester in FR1 and FR2 were not measurably different from thermal decomposition products from the poly(propylene) and polyester in the control HVAC module [3]. Thus, thermal decomposition of the polymers yielded the same types of products. Thermal

decomposition of these polymers and volatilization of the thermal decomposition products occurred at similar rates in the control and the two experimental HVAC modules. The observed reductions in the oxygen consumption rates, carbon dioxide release rates, and heat release rates and increases in carbon monoxide release rate, total hydrocarbon release rate, and smoke release rate indicate that oxidization of the thermal decomposition products in the flame was less efficient in tests of FR1 and FR2 than in the test of the control HVAC module.

REFERENCES

1. G. Heskestad. A Fire Products Collector for Calorimetry into the MW Range, Technical Report J.I. OC2E1.RA. Factory Mutual Research Corporation, Norwood, MA. June, 1981.

2. Archibald Tewarson. "Generation of Heat and Chemical Compounds in Fires" Section 3/Chapter 4, SFPE Handbook of Fire Protection Engineering, 2nd Edition, 1995, pp. 3:53-124.

3. Jeffrey Santrock. Chemical analysis of thermal decomposition products from polymers containing flame retardant chemical additives.

APPENDIX A
Fire Products Collector Data
Heptane Only

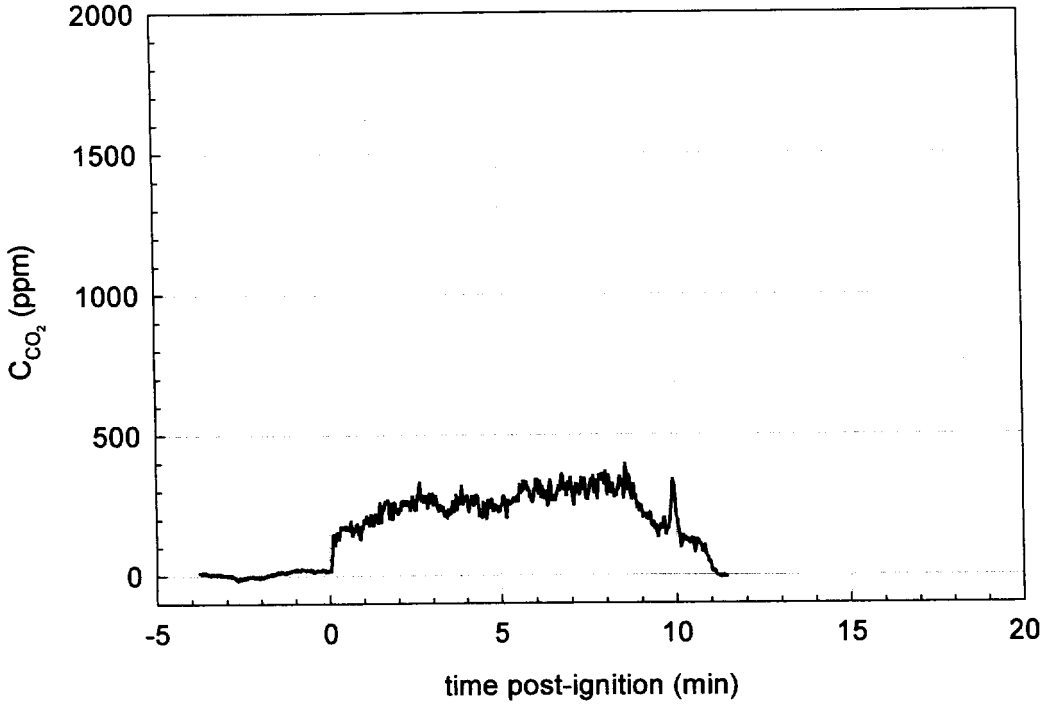

Plot A1. Carbon dioxide concentration measured in the fire products collector with heptane only.

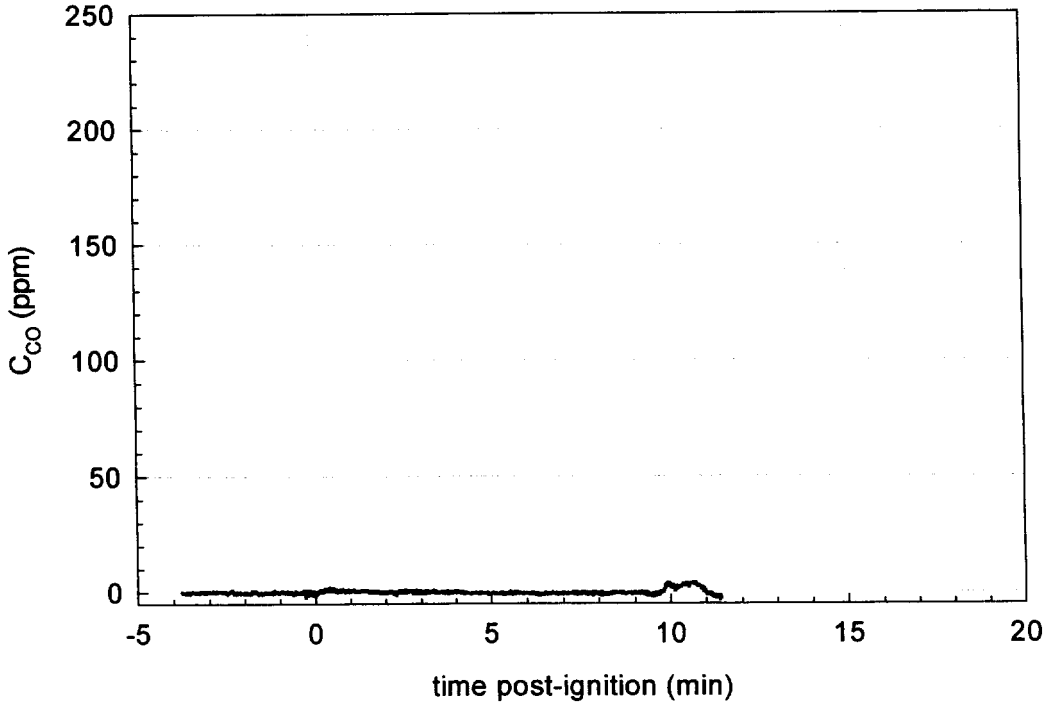

Plot A2. Carbon monoxide concentration measured in the fire products collector with heptane only.

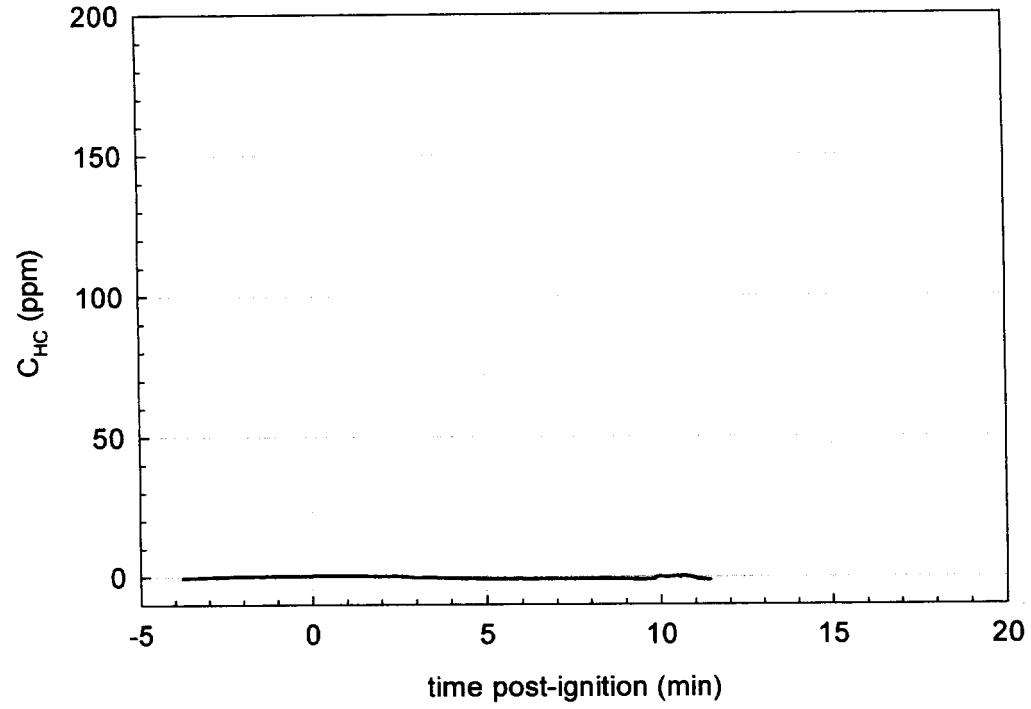

Plot A3. Hydrocarbon concentration measured in the fire products collector with heptane only.

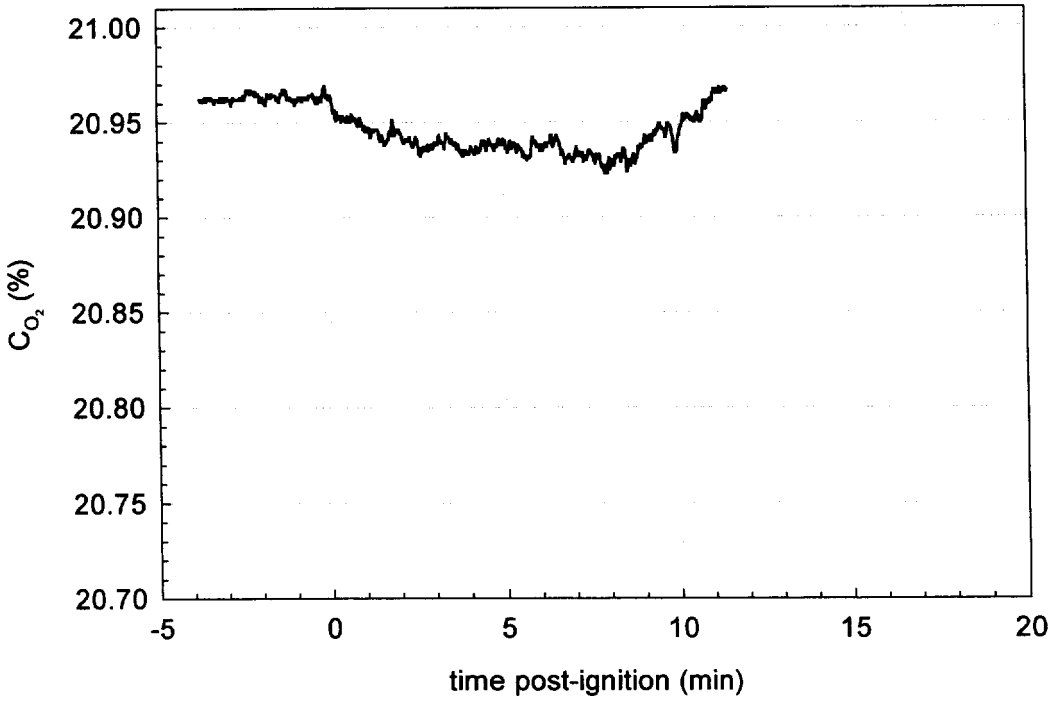

Plot A4. Oxygen concentration measured in the fire products collector with heptane only.

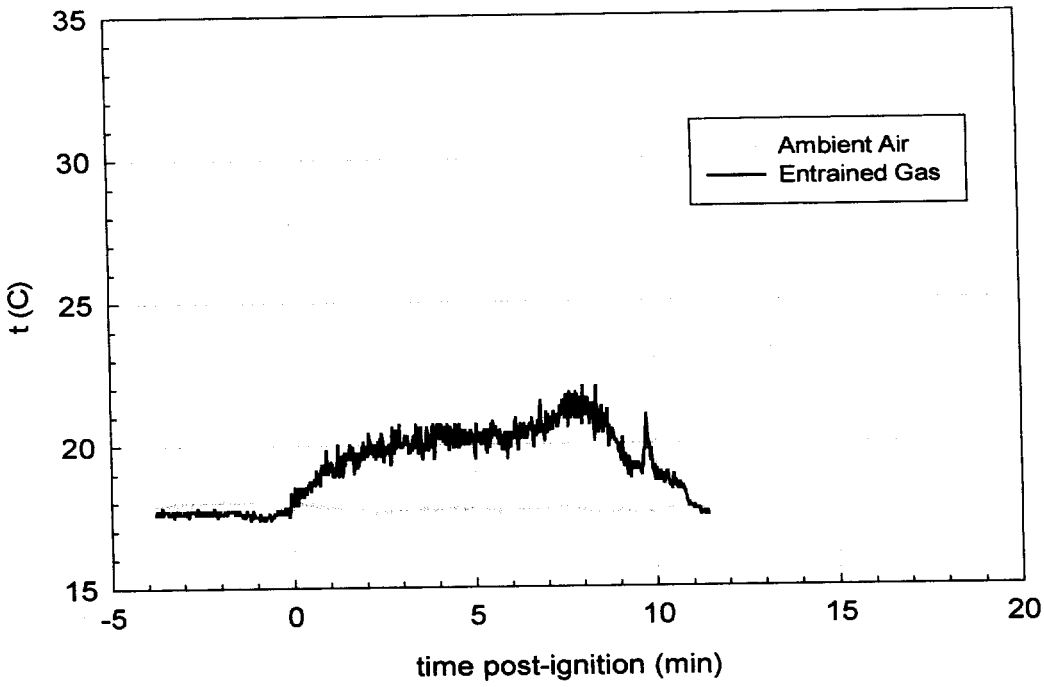

Plot A5. Temperature of ambient air and gas entrained in the fire products collector with heptane only.

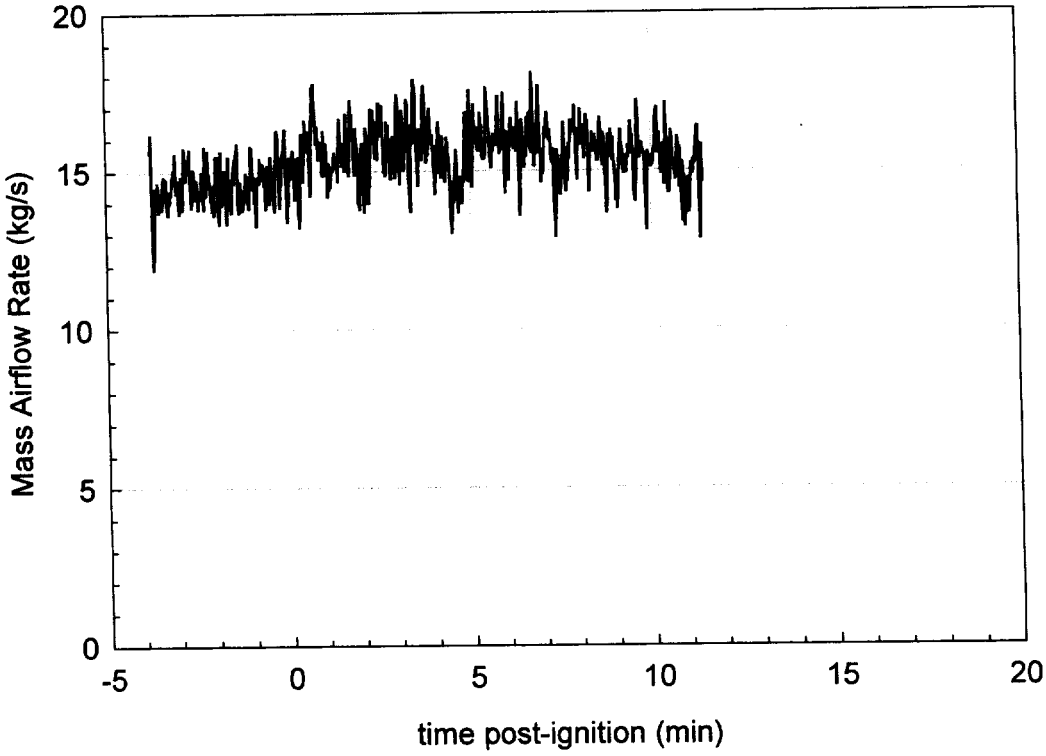

Plot A6. Mass airflow rate into the fire products collector with heptane only.

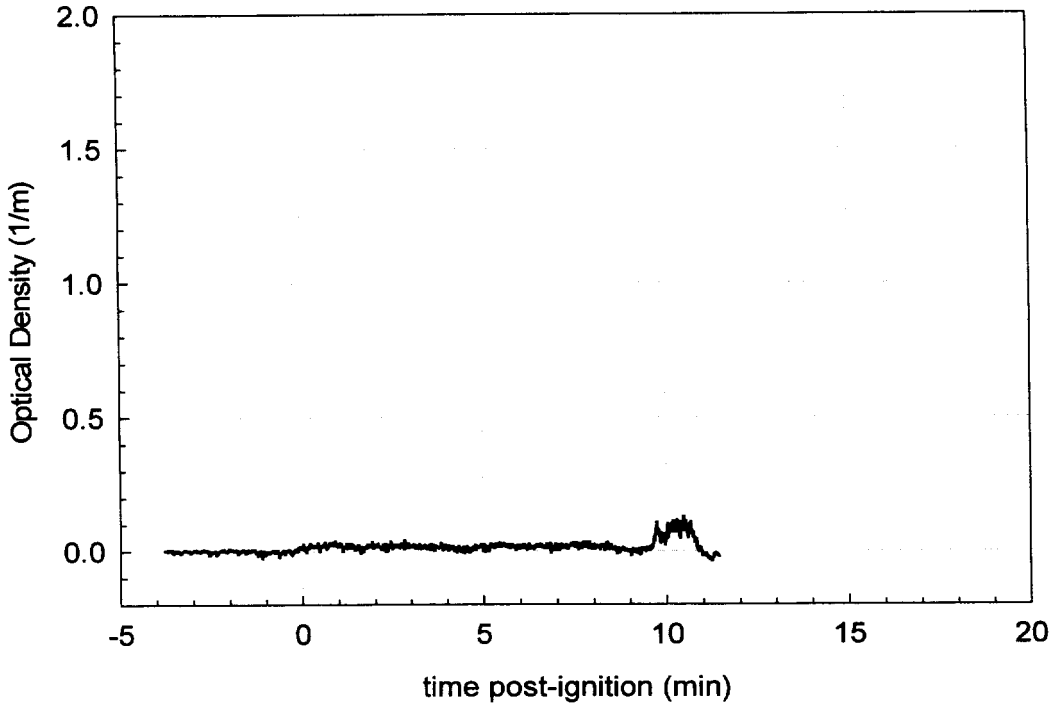

Plot A7. Optical density of air entrained into the fire products collector at λ = 0.4679 μm (blue) with heptane only.

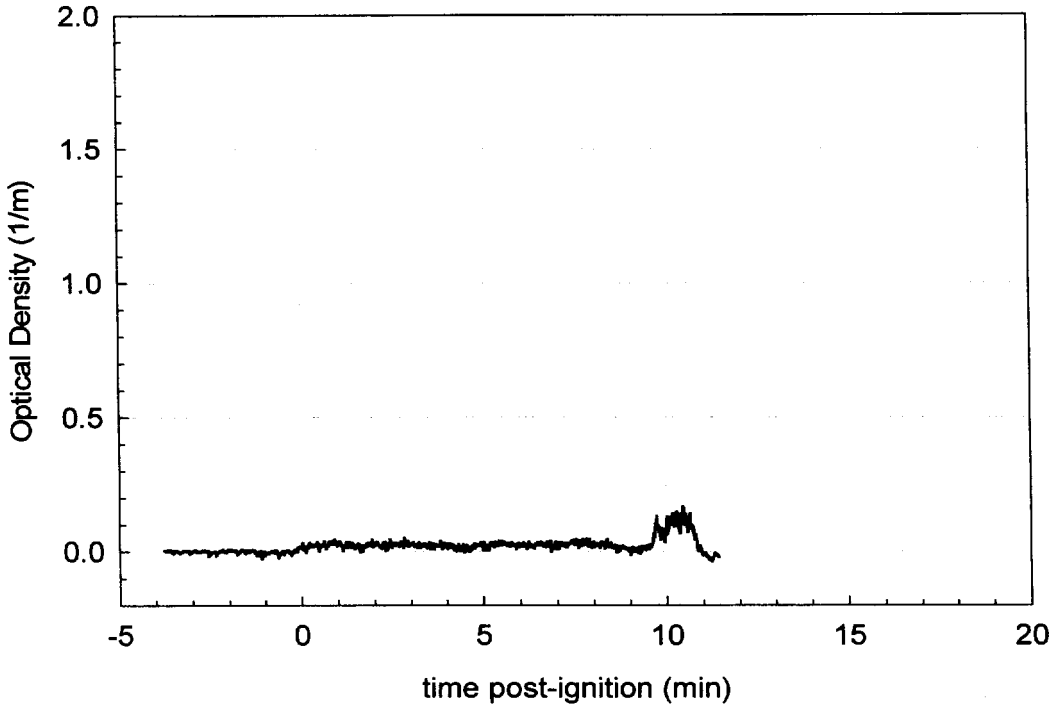

Plot A8. Optical density of air entrained into the fire products collector at λ = 0.6328 μm (red) with heptane only.

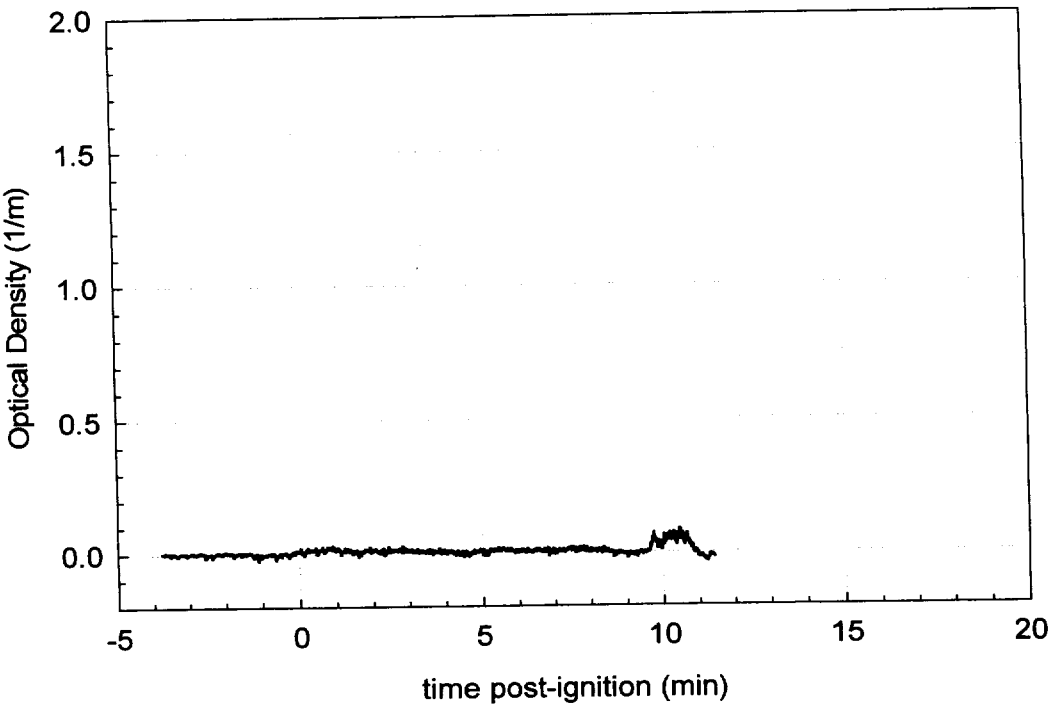

Plot A9. Optical density of air entrained into the fire products collector at λ = 1.06 μm (infrared) with heptane only.

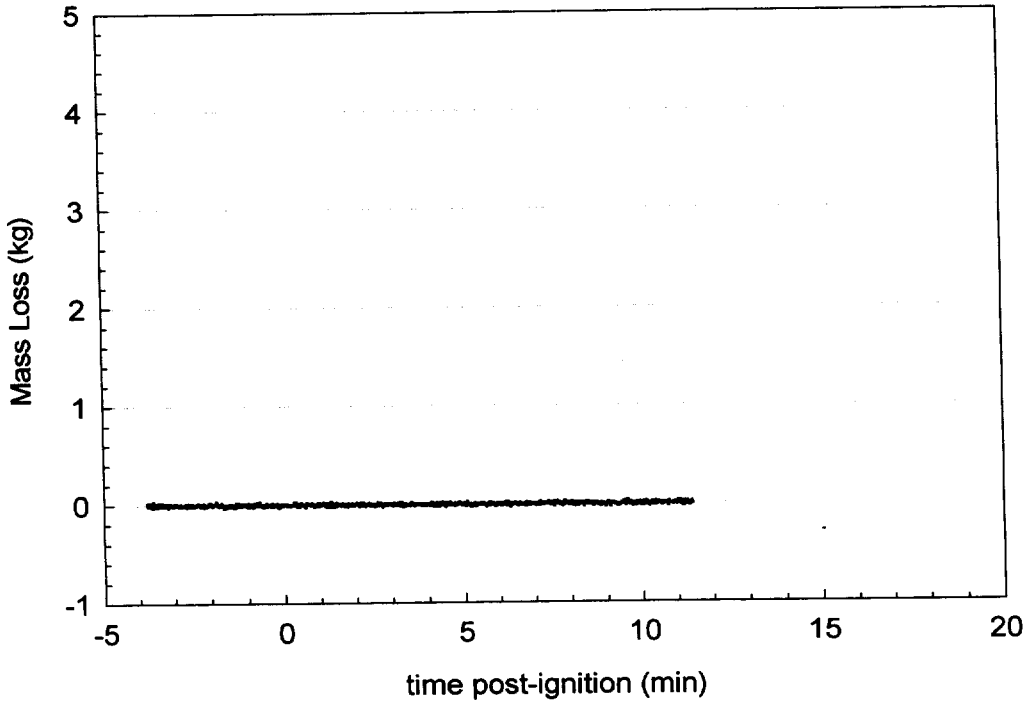

Plot A10. Mass loss from the HVAC module stand (no HVAC module) with heptane only.

APPENDIX B
Fire Products Collector Data
Control HVAC Module

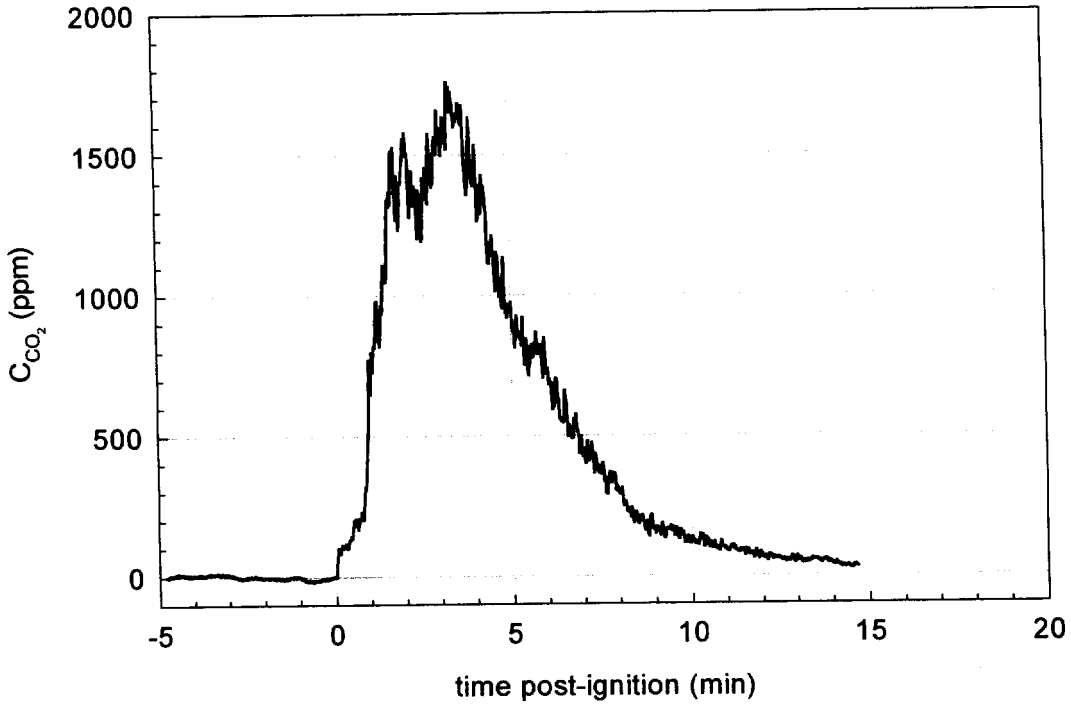

Plot B1. Carbon dioxide concentration measured in the fire products collector with the control HVAC module.

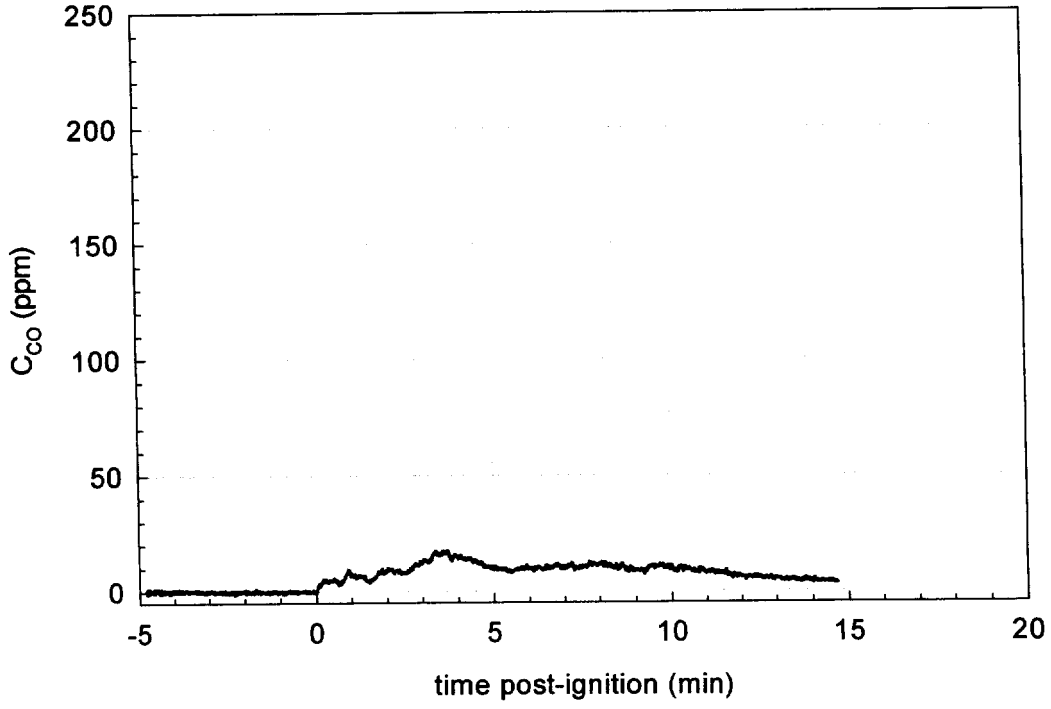

Plot B2. Carbon monoxide concentration measured in the fire products collector with the control HVAC module.

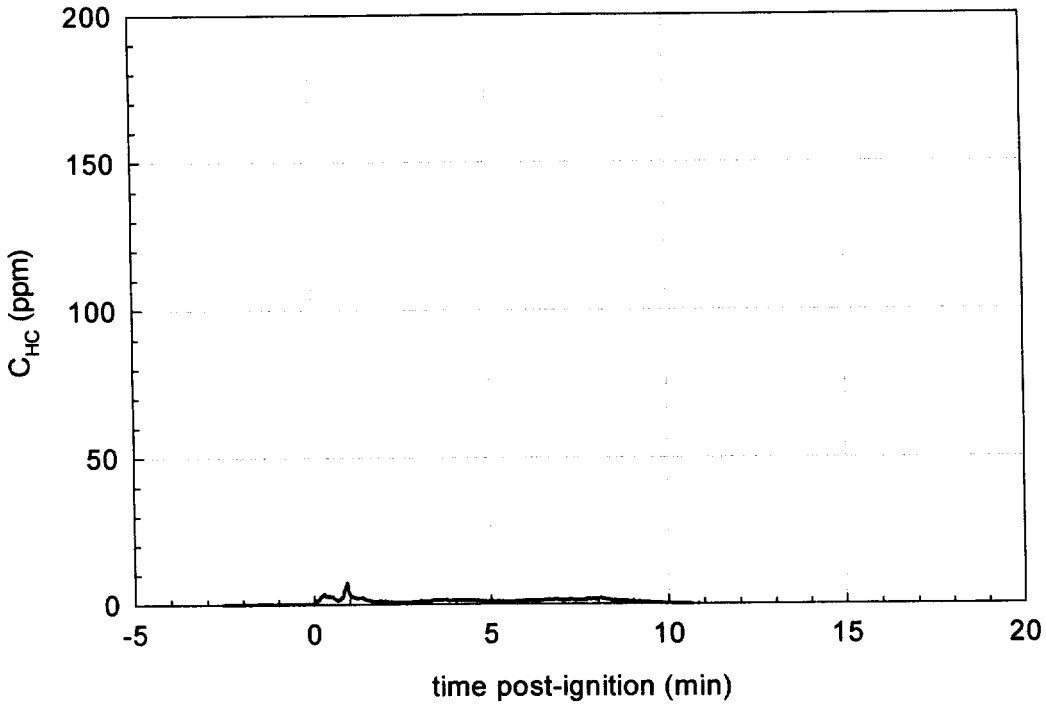

Plot B3. Hydrocarbon concentration measured in the fire products collector with the control HVAC module.

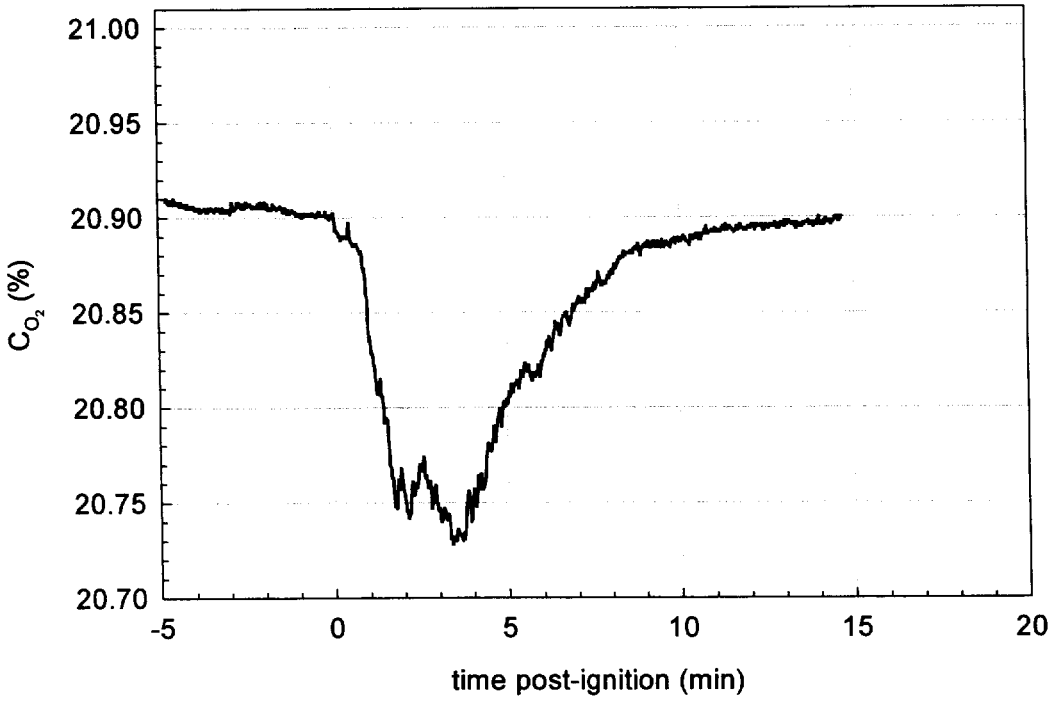

Plot B4. Oxygen concentration measured in the fire products collector the control HVAC module.

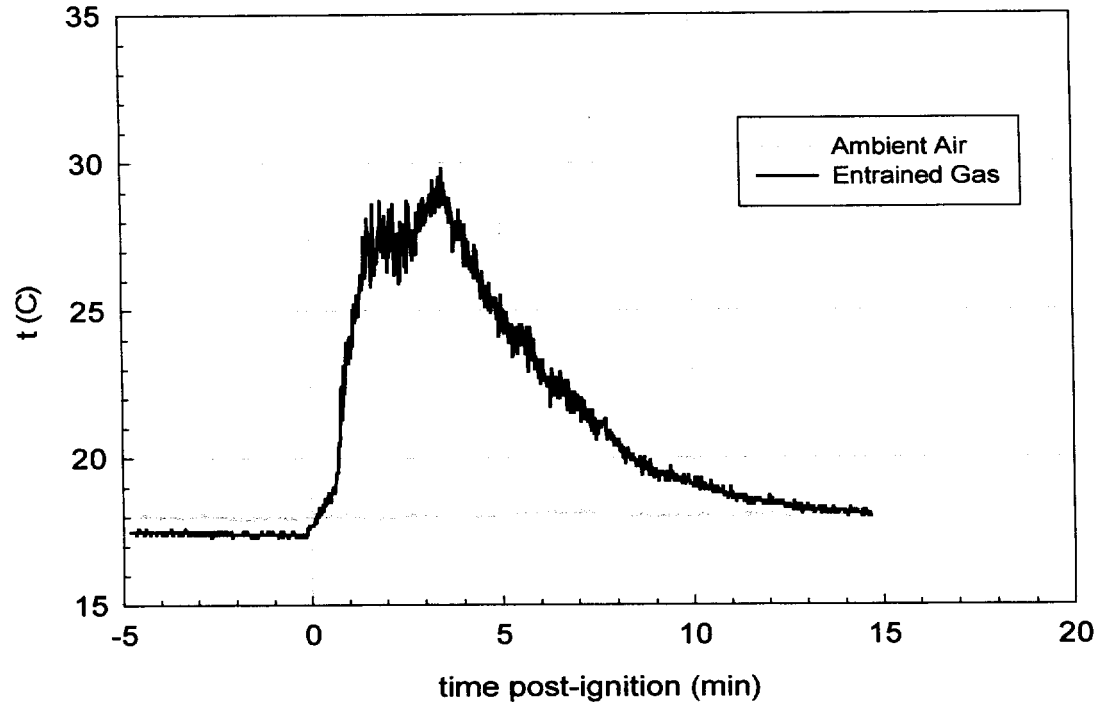

Plot B5. Temperature of ambient air and gas entrained in the fire products collector with the control HVAC module.

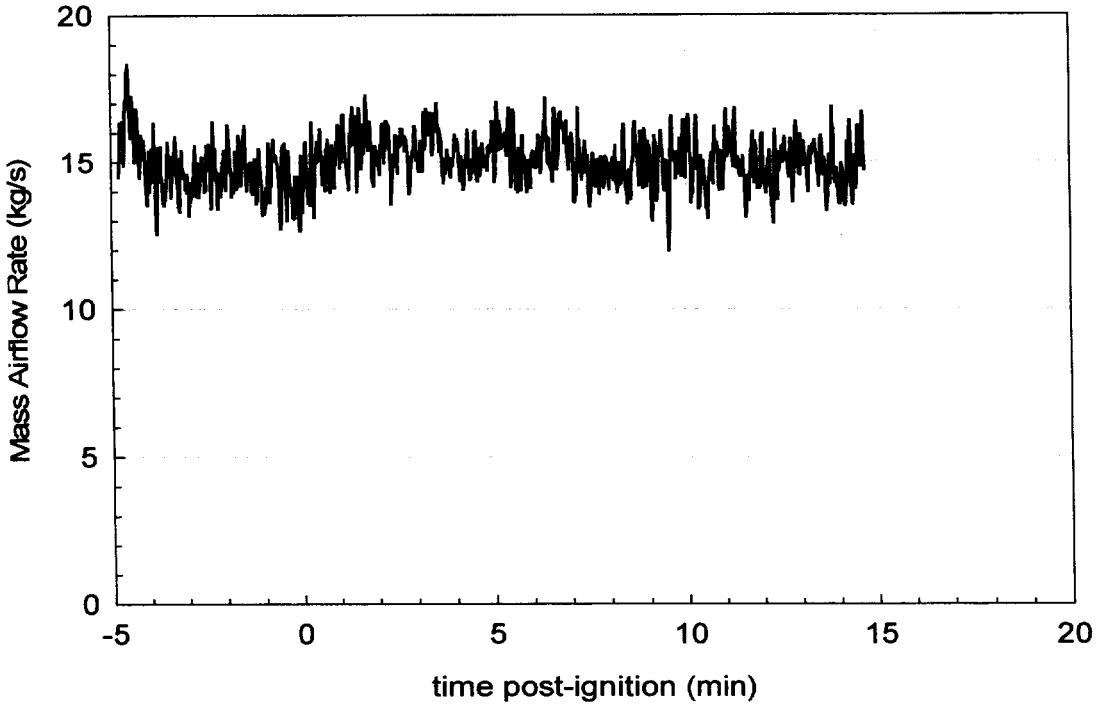

Plot B6. Mass airflow rate into the fire products collector the control HVAC module.

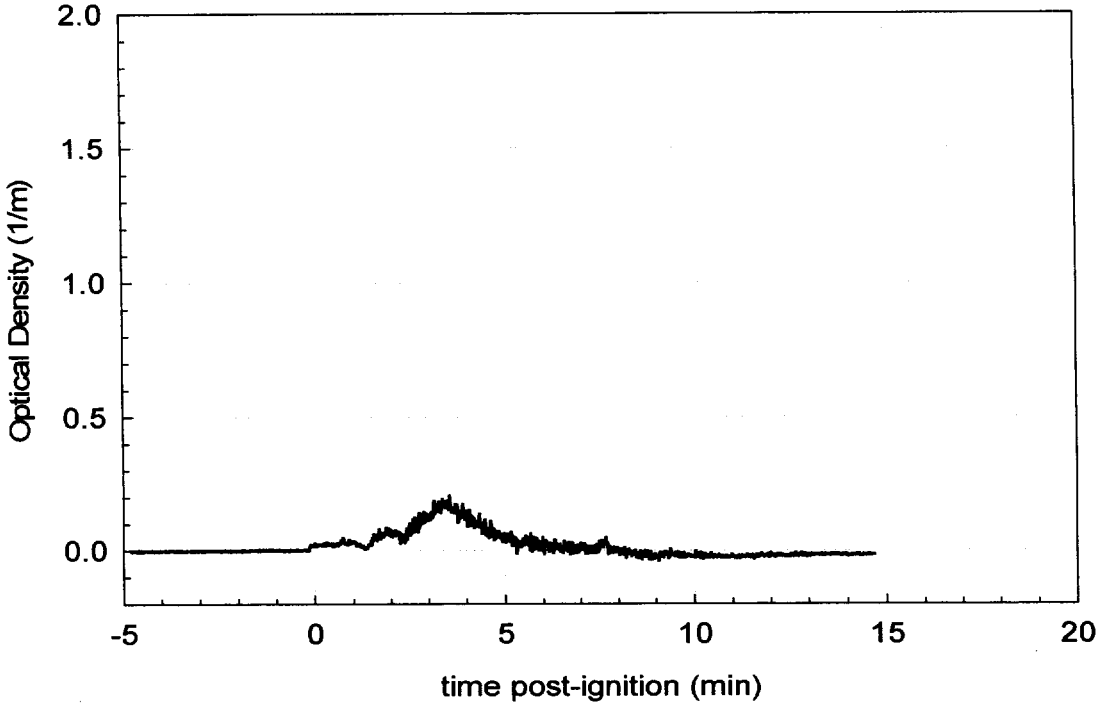

Plot B7. Optical density of air entrained into the fire products collector at λ = 0.4679 μm (blue) with the control HVAC module.

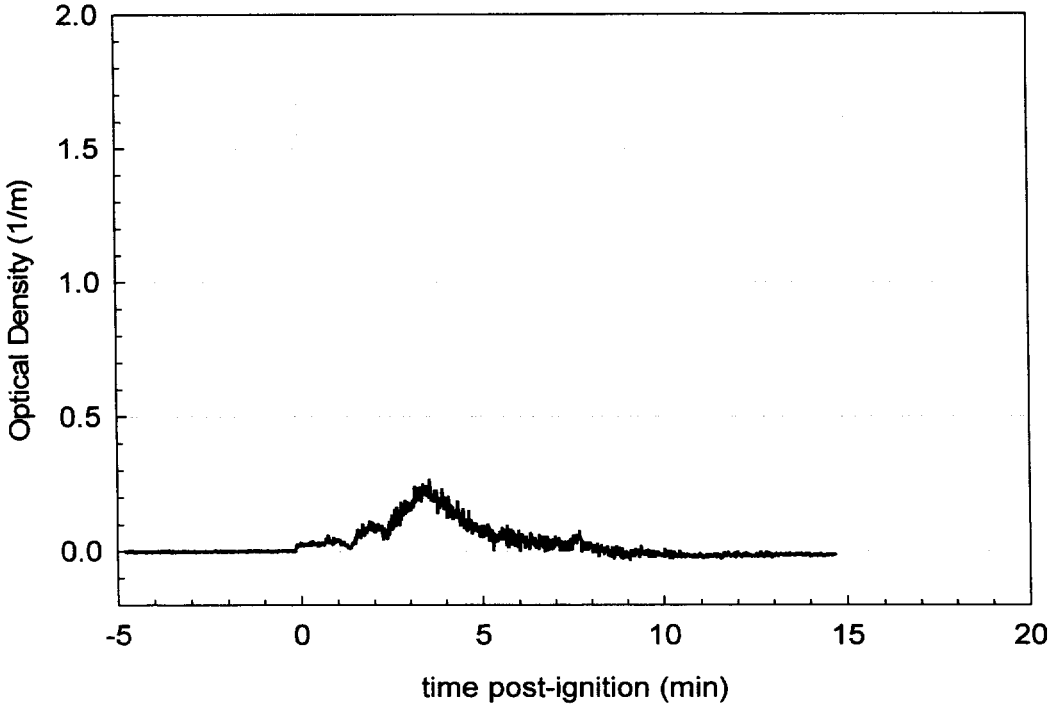

Plot B8. Optical density of air entrained into the fire products collector at λ = 0.6328 μm (red) with the control HVAC module.

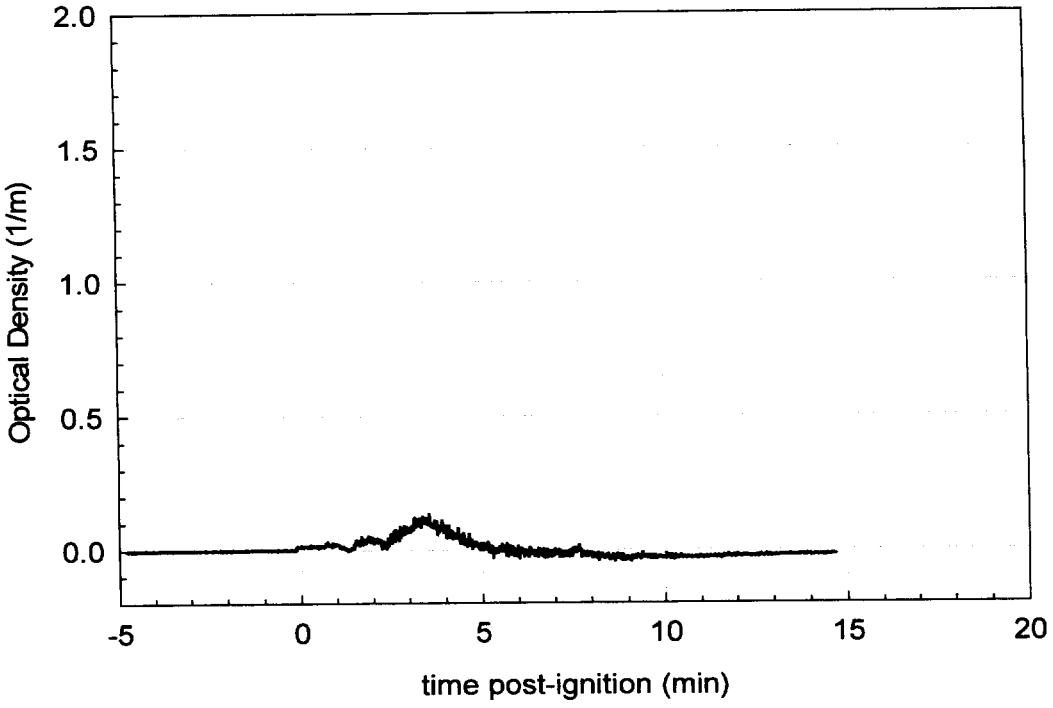

Plot B9. Optical density of air entrained into the fire products collector at λ = 1.06 μm (infrared) with the control HVAC module.

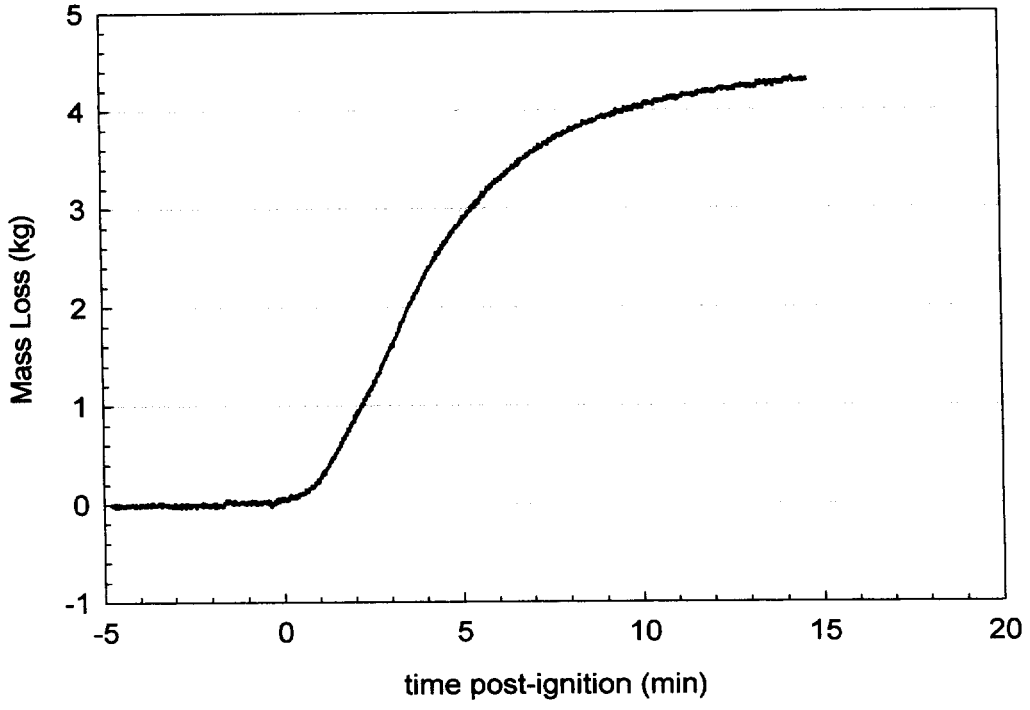

Plot B10. Mass loss from the control HVAC module.

APPENDIX C
Fire Products Collector Data
FR1 HVAC Module

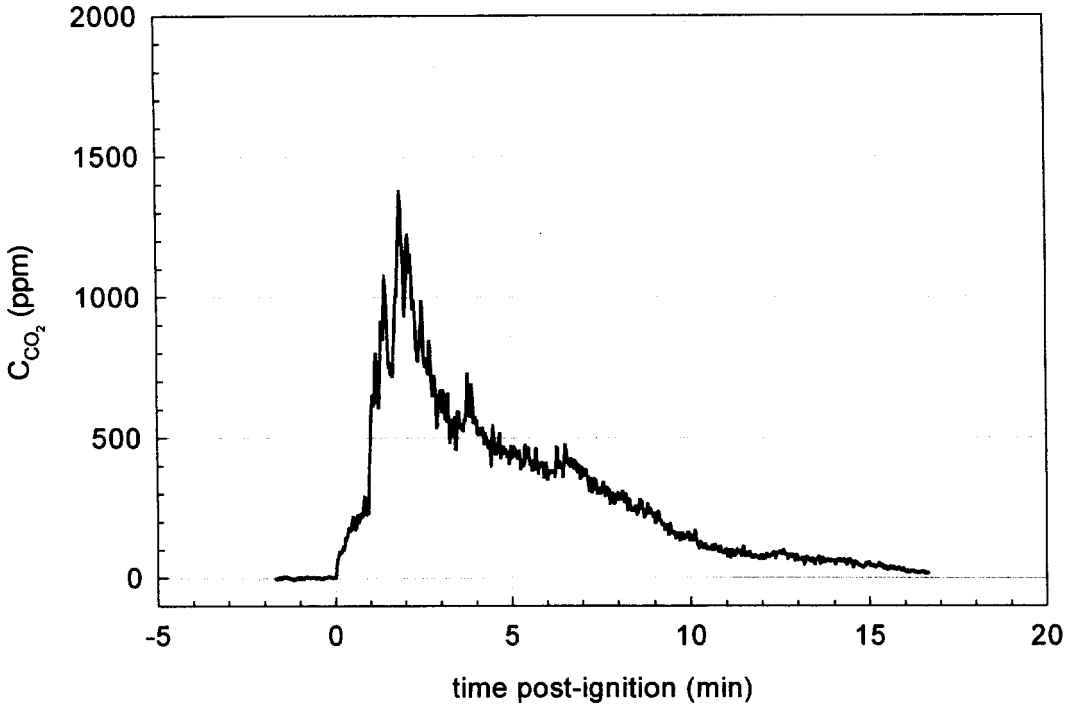

Plot C1. Carbon dioxide concentration measured in the fire products collector with the FR1 HVAC module.

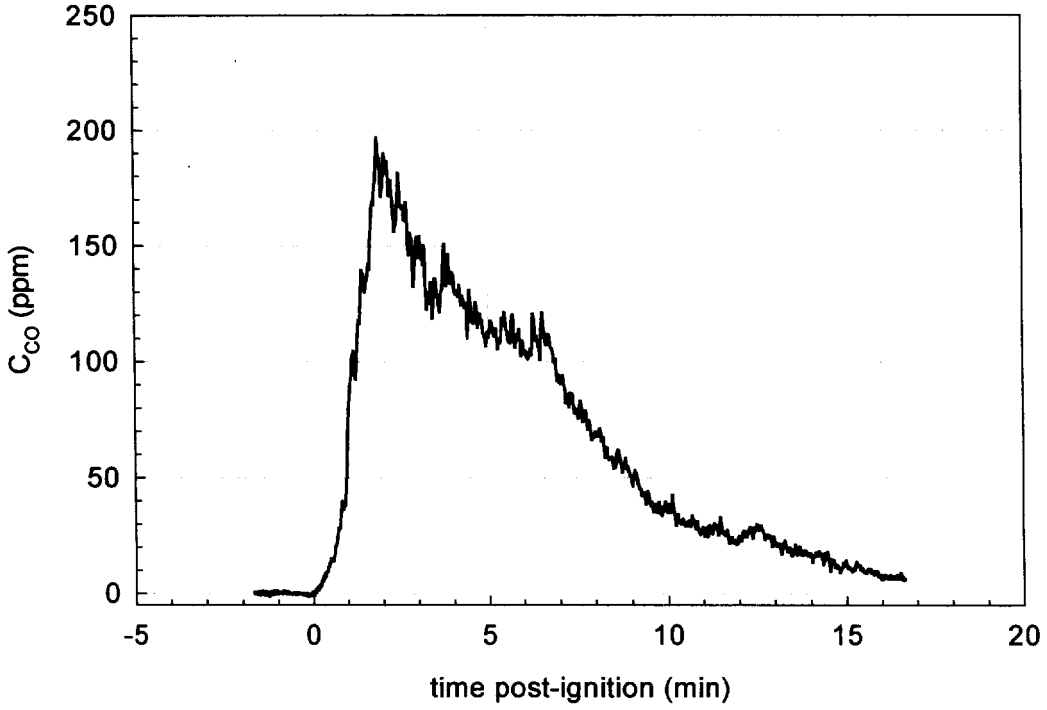

Plot C2. Carbon monoxide concentration measured in the fire products collector with the FR1 HVAC module.

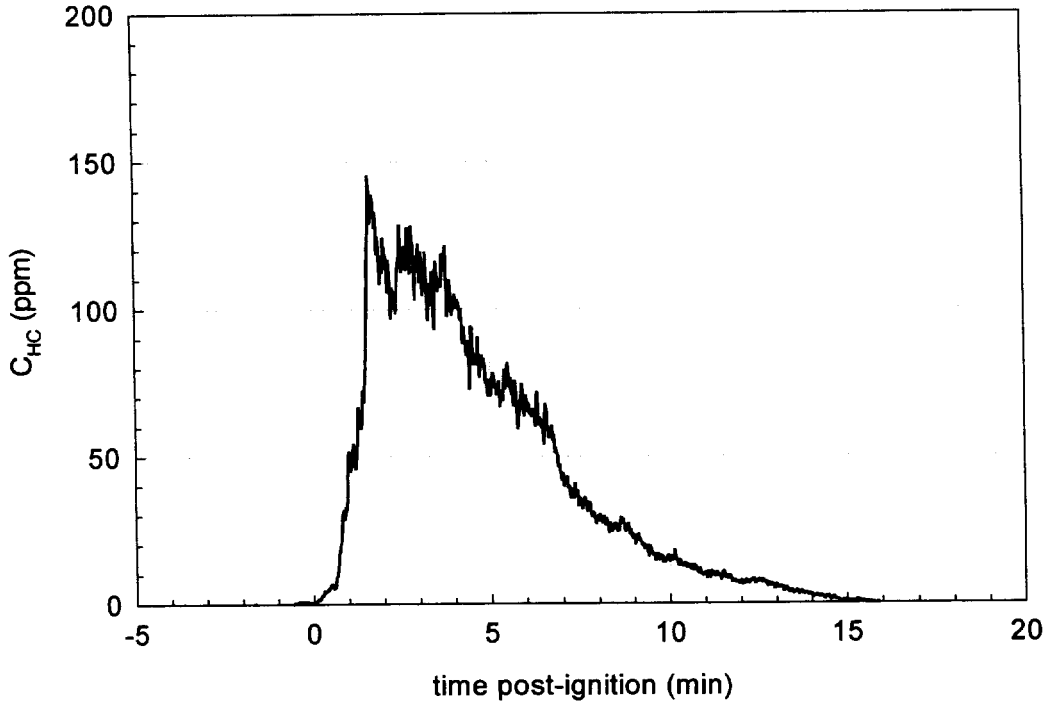

Plot C3. Hydrocarbon concentration measured in the fire products collector with the FR1 HVAC module.

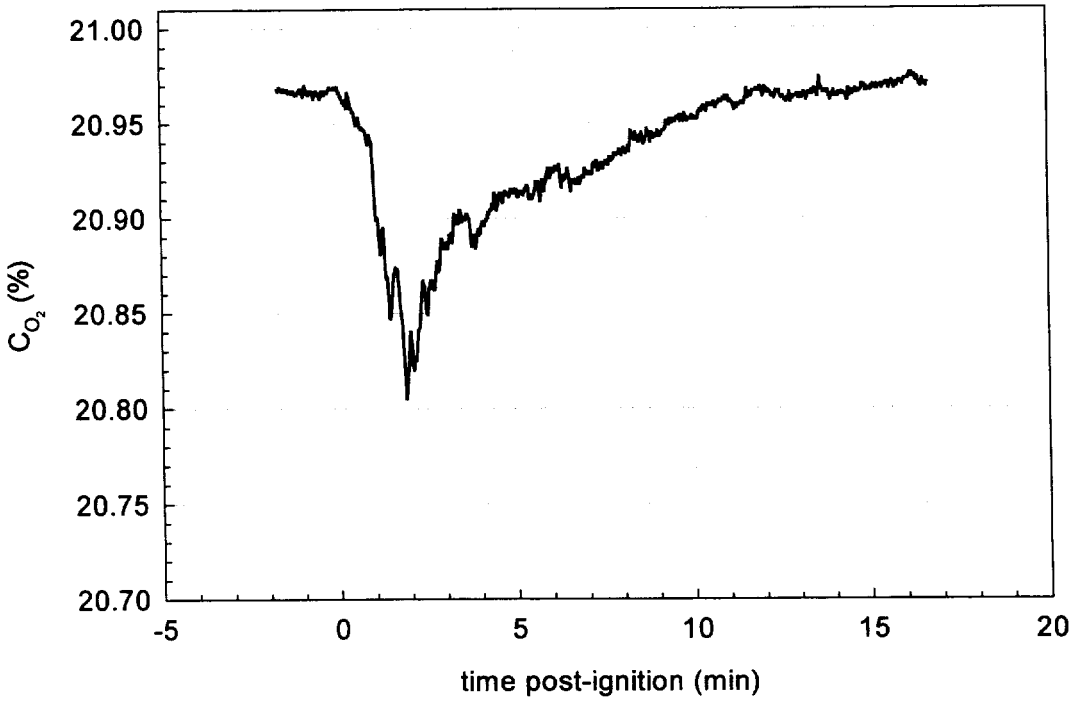

Plot C4. Oxygen concentration measured in the fire products collector the FR1 HVAC module.

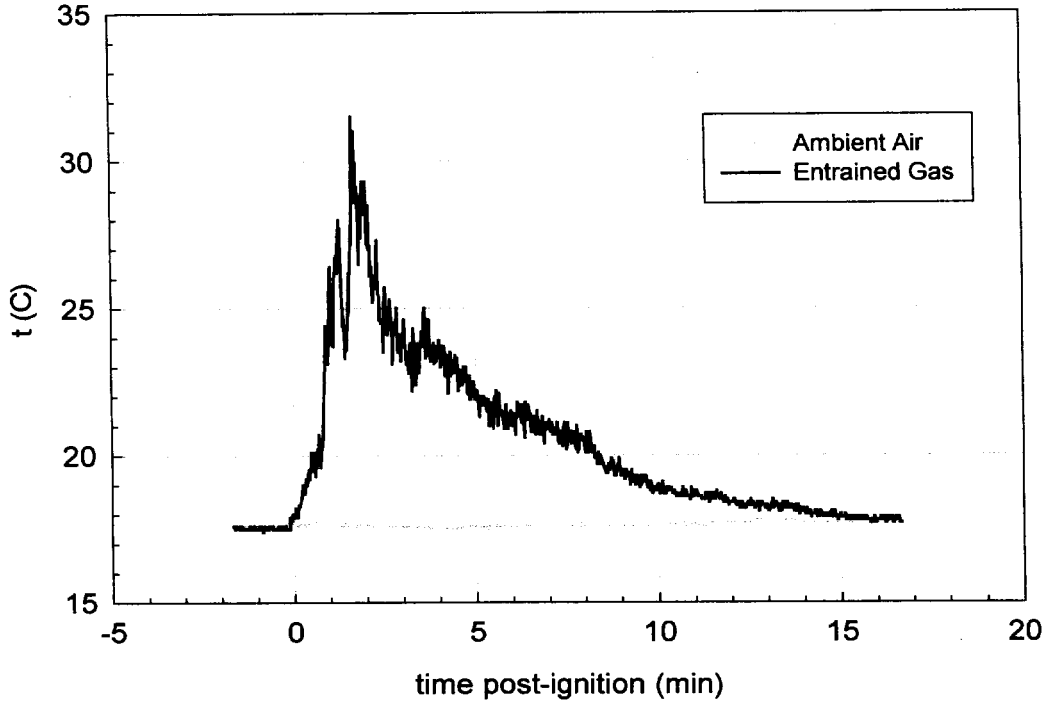

Plot C5. Temperature of ambient air and gas entrained in the fire products collector with the FR1 HVAC module.

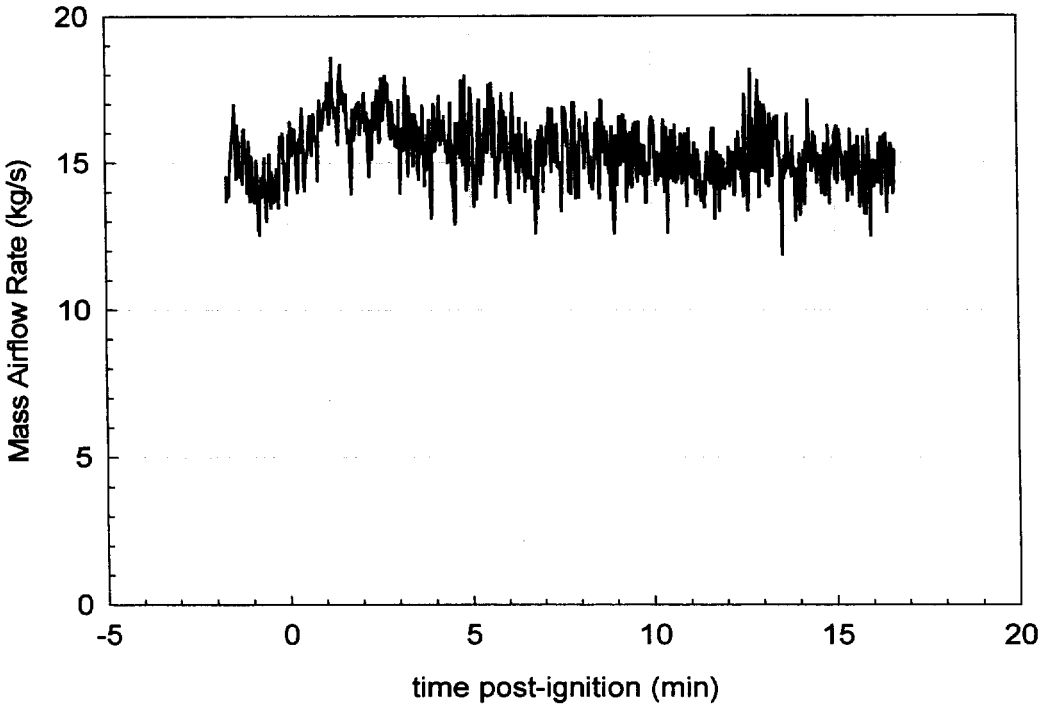

Plot C6. Mass airflow rate into the fire products collector the FR1 HVAC module.

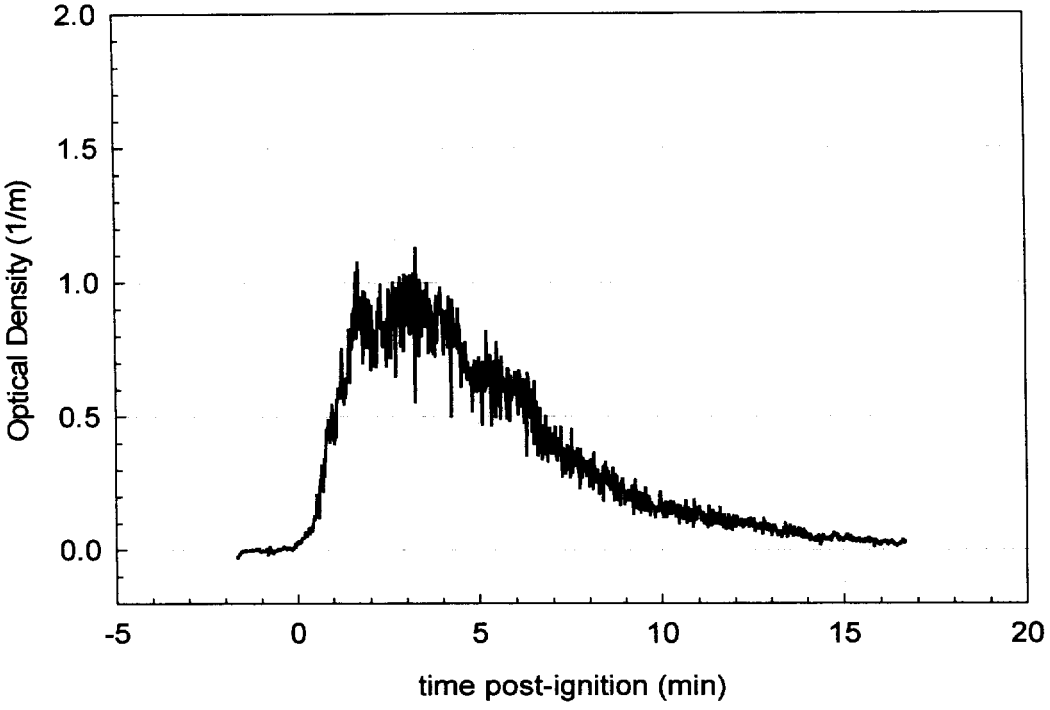

Plot C7. Optical density of air entrained into the fire products collector at λ = 0.4679 μm (blue) with the FR1 HVAC module.

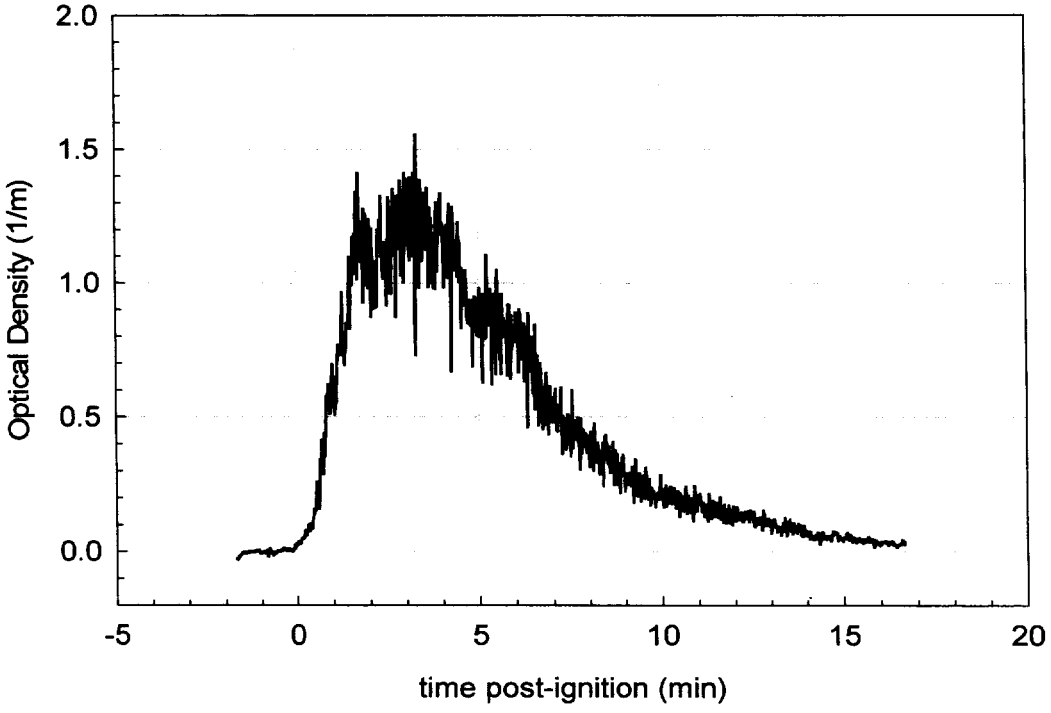

Plot C8. Optical density of air entrained into the fire products collector at λ = 0.6328 μm (red) with the FR1 HVAC module.

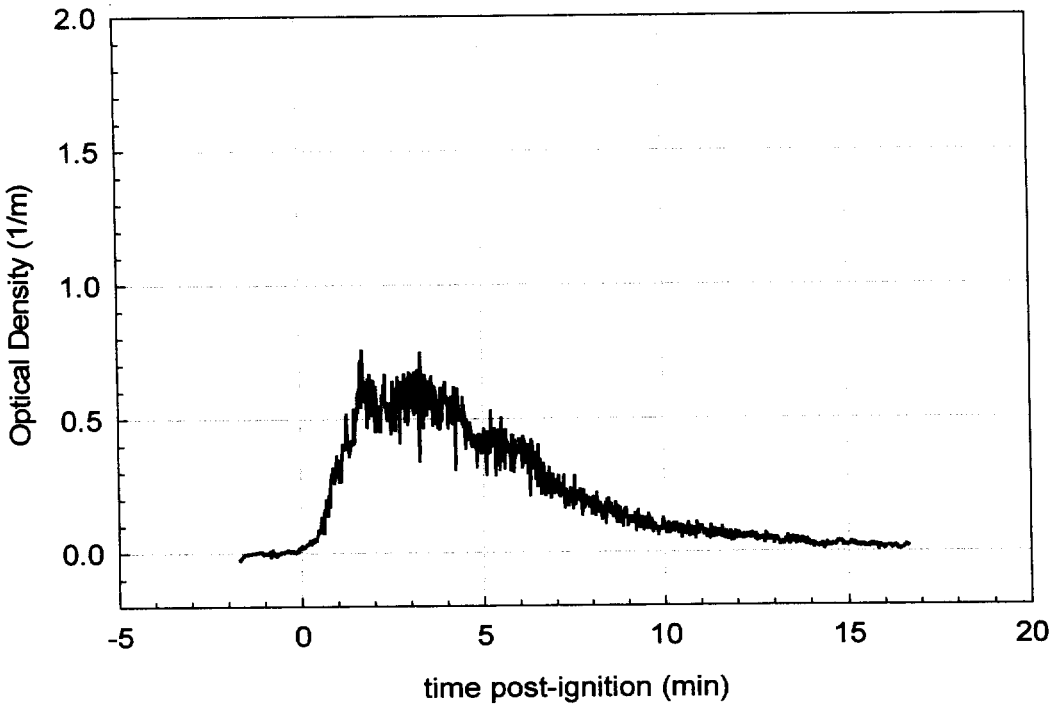

Plot C9. Optical density of air entrained into the fire products collector at λ = 1.06 μm (infrared) with the FR1 HVAC module.

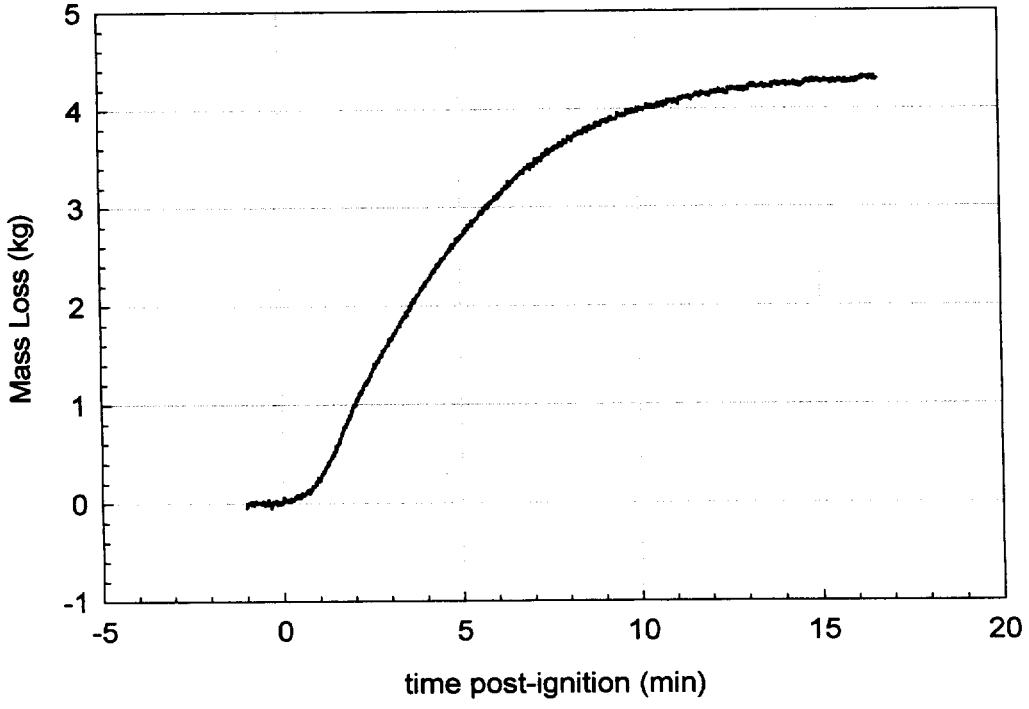

Plot C10. Mass loss from the FR1 HVAC module.

APPENDIX D
Fire Products Collector Data
FR2 HVAC Module

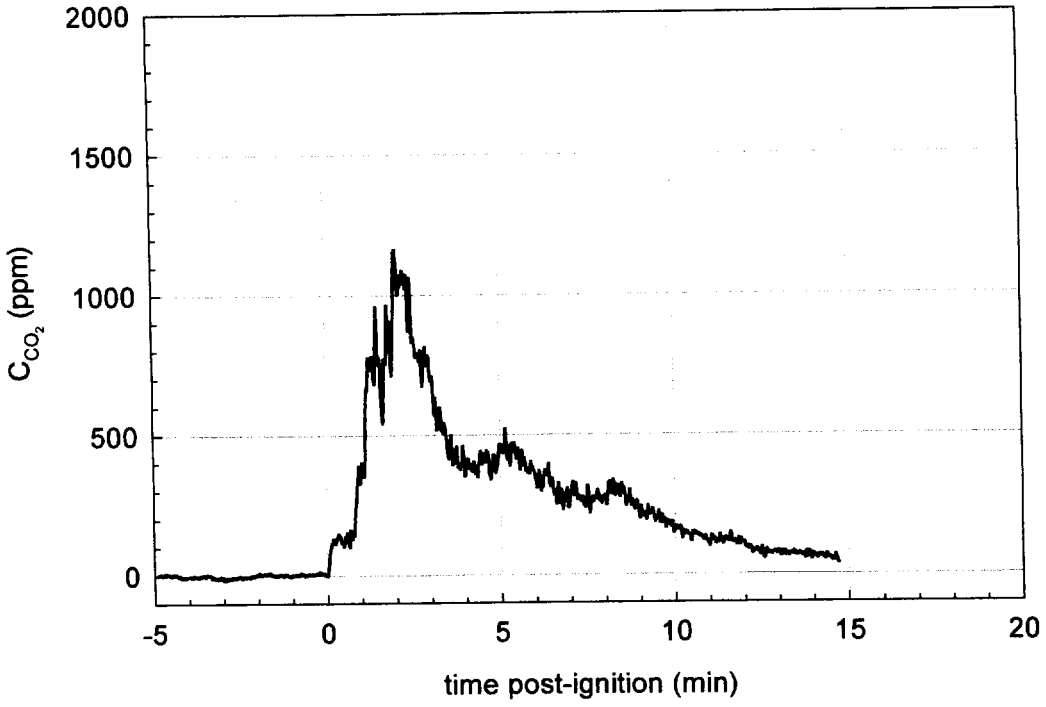

Plot D1. Carbon dioxide concentration measured in the fire products collector with the FR2 HVAC module.

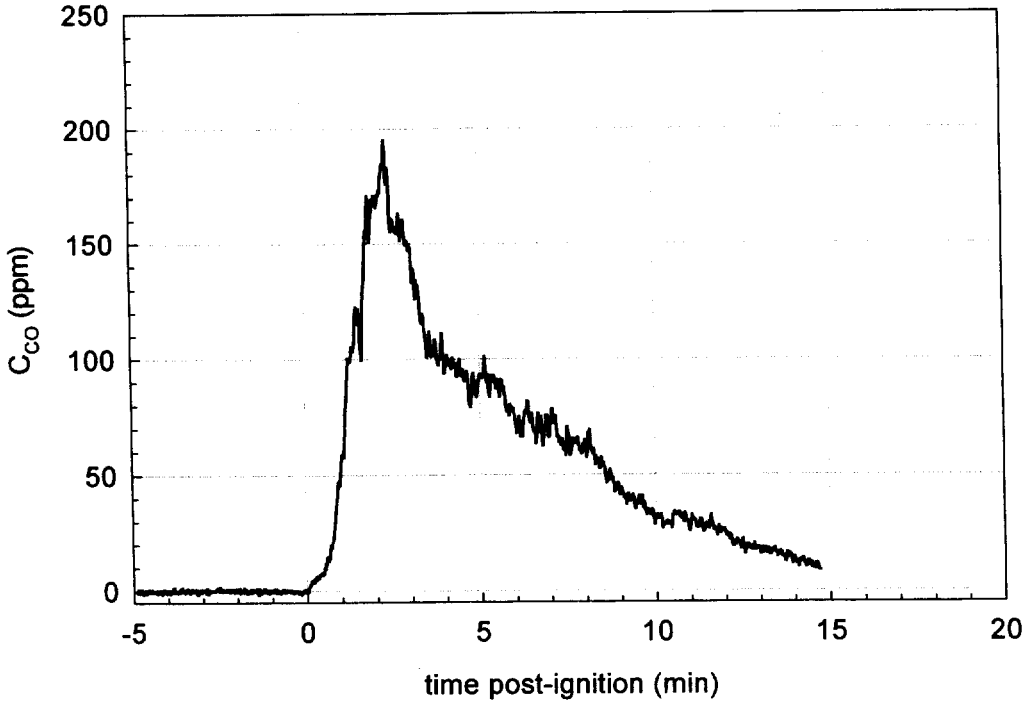

Plot D2. Carbon monoxide concentration measured in the fire products collector with the FR2 HVAC module.

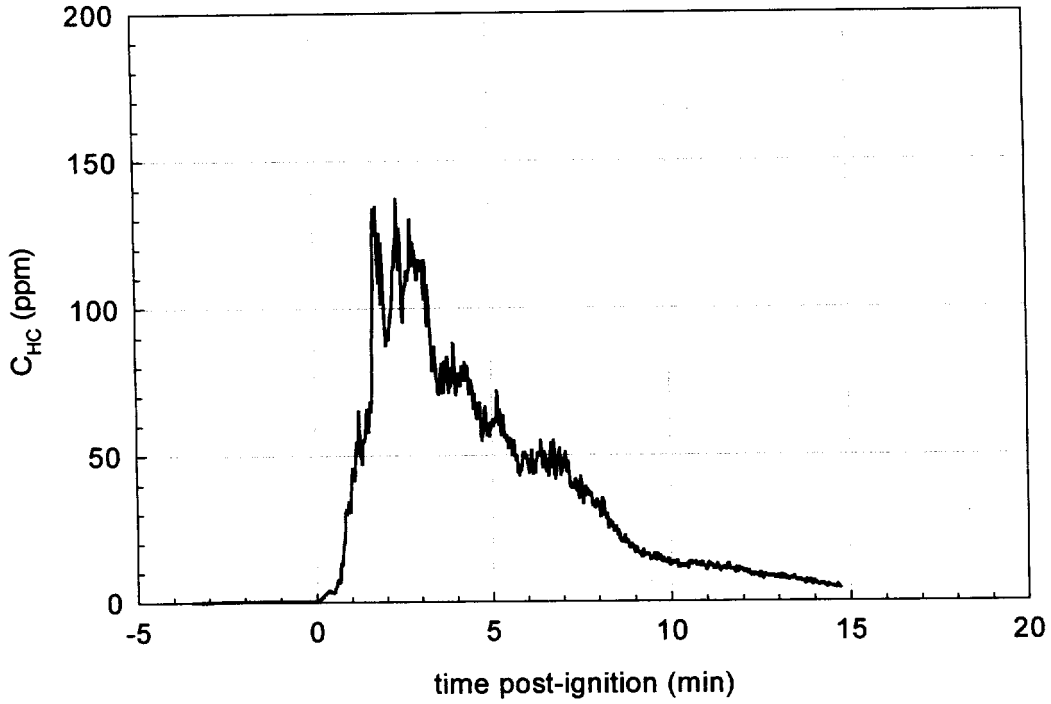

Plot D3. Hydrocarbon concentration measured in the fire products collector with the FR2 HVAC module.

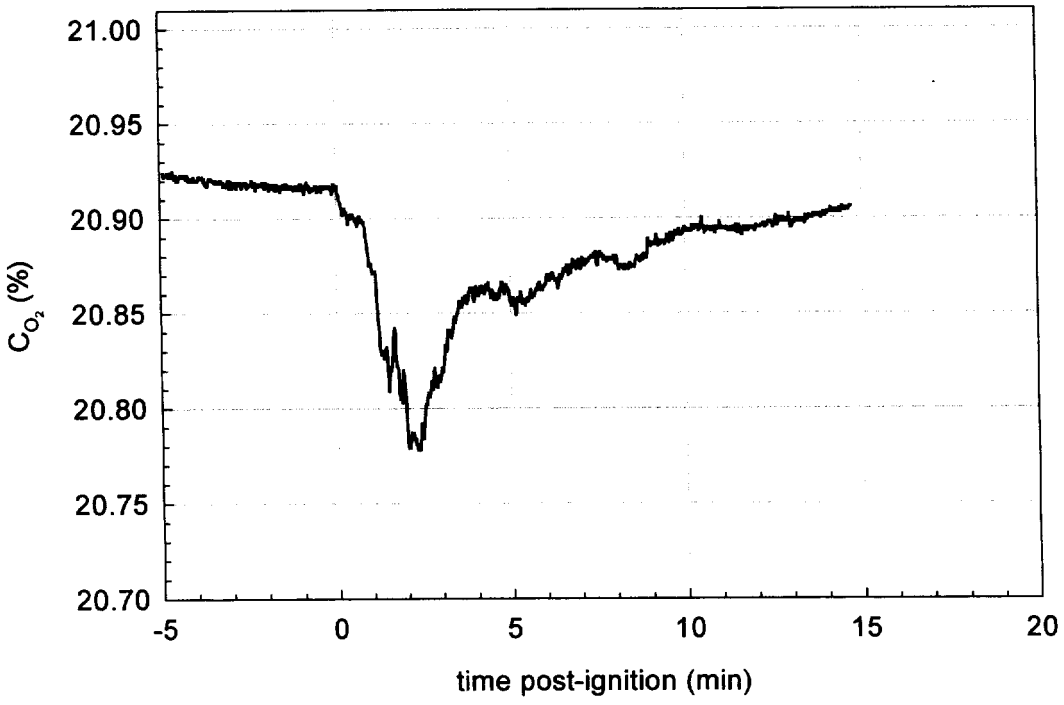

Plot D4. Oxygen concentration measured in the fire products collector the FR2 HVAC module.

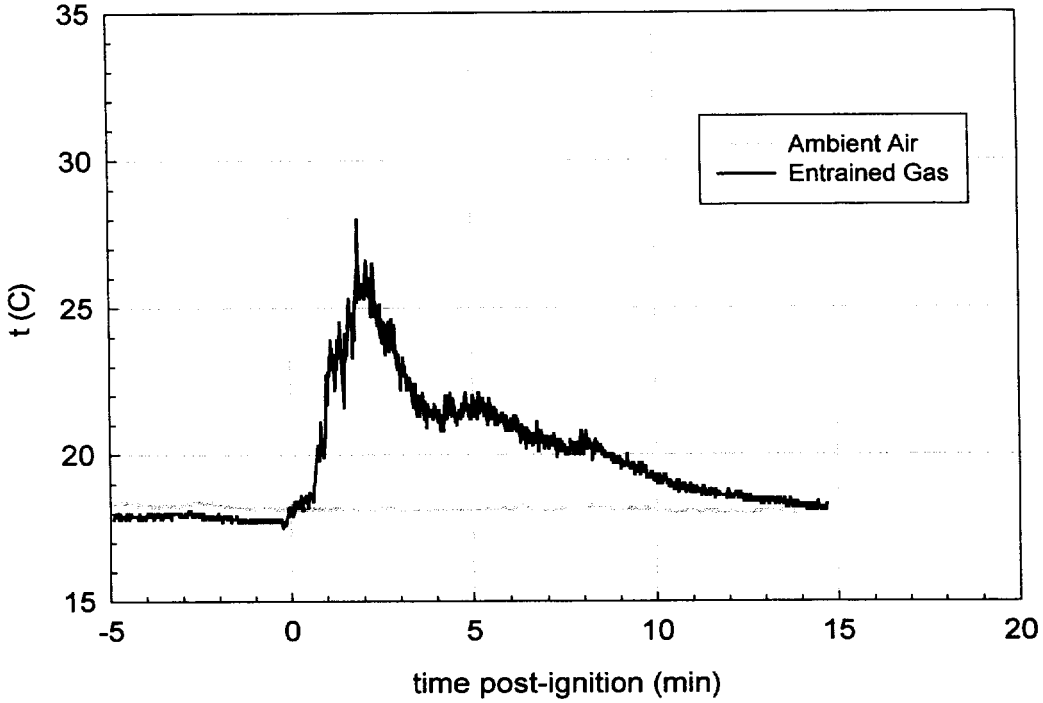

Plot D5. Temperature of ambient air and gas entrained in the fire products collector with the FR2 HVAC module.

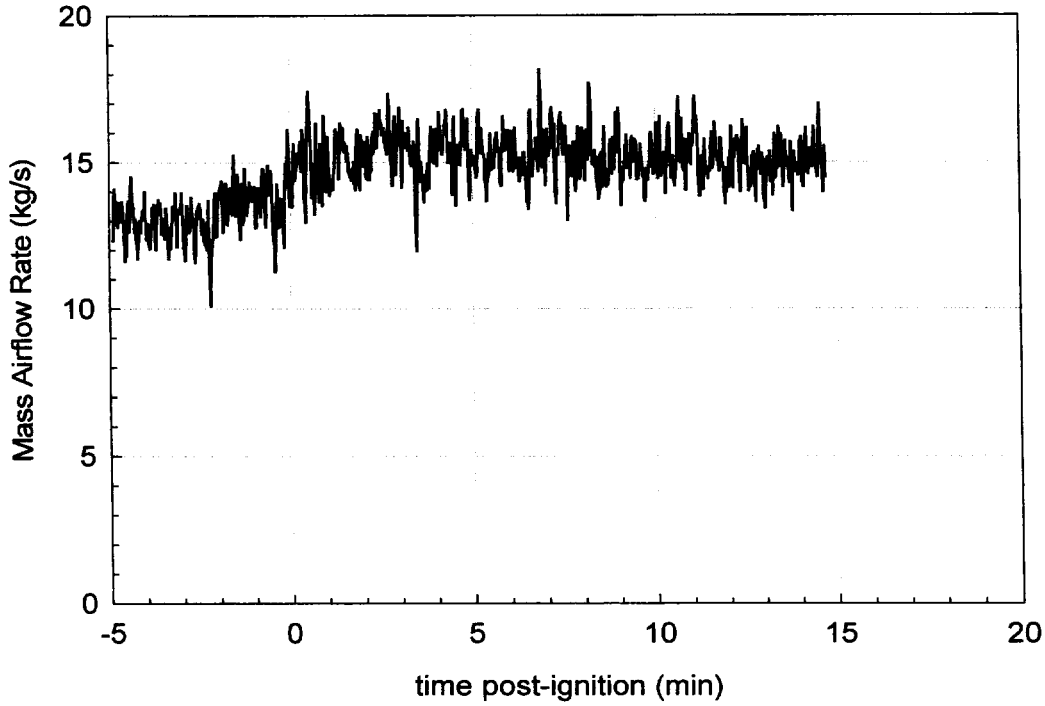

Plot D6. Mass airflow rate into the fire products collector the FR2 HVAC module.

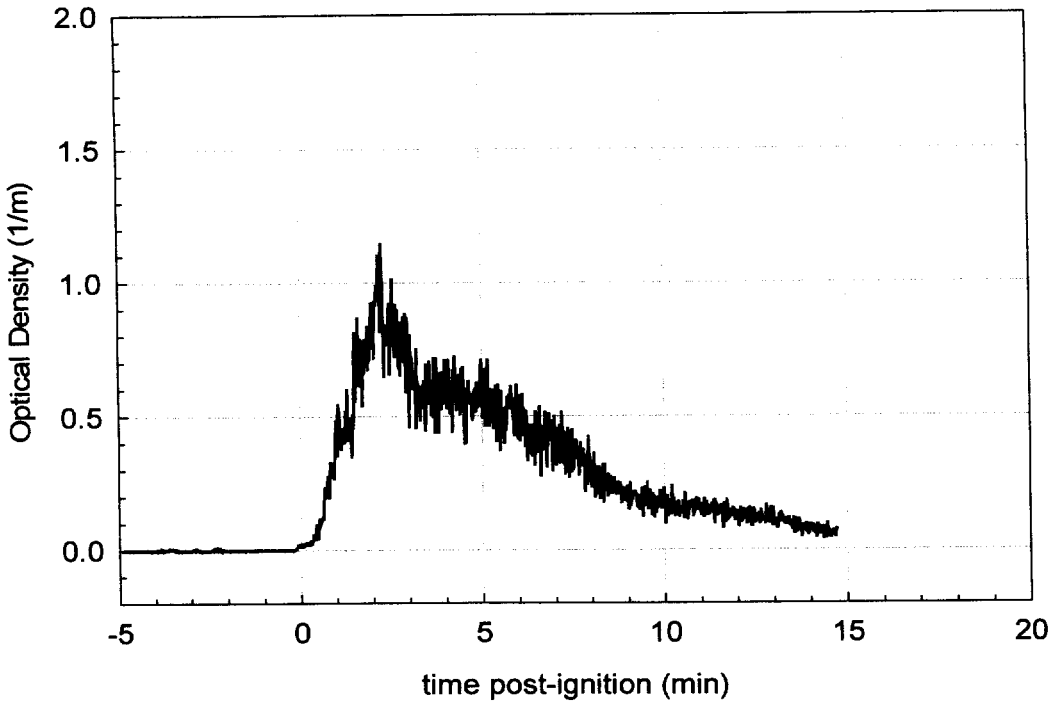

Plot D7. Optical density of air entrained into the fire products collector at λ = 0.4679 μm (blue) with the FR2 HVAC module.

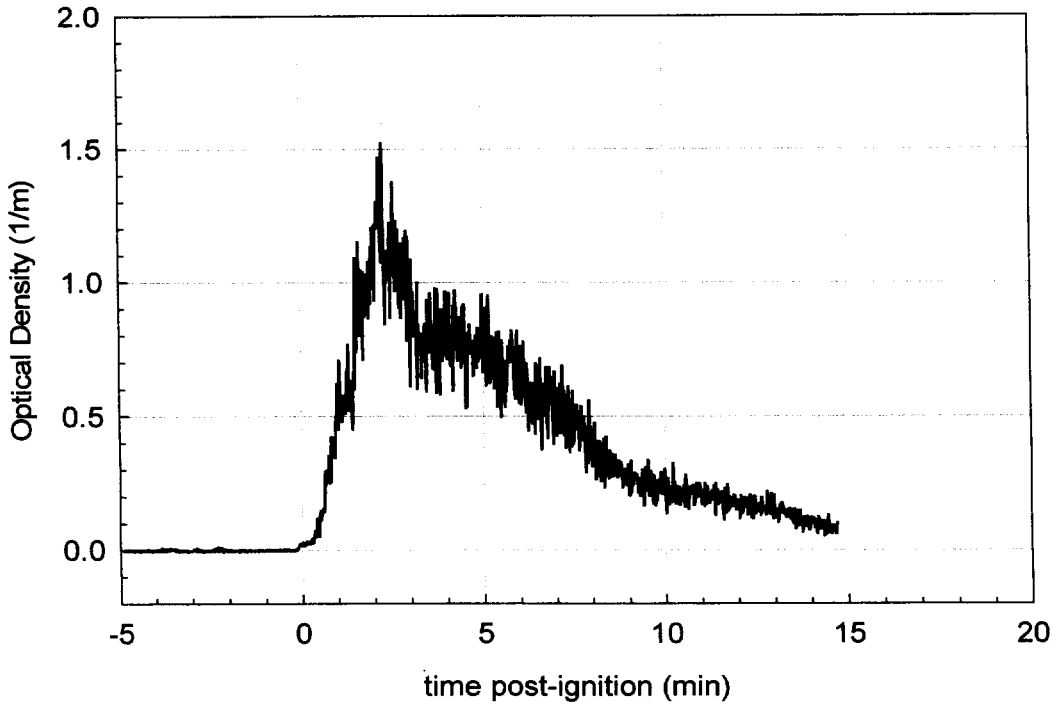

Plot D8. Optical density of air entrained into the fire products collector at λ = 0.6328 μm (red) with the FR2 HVAC module.

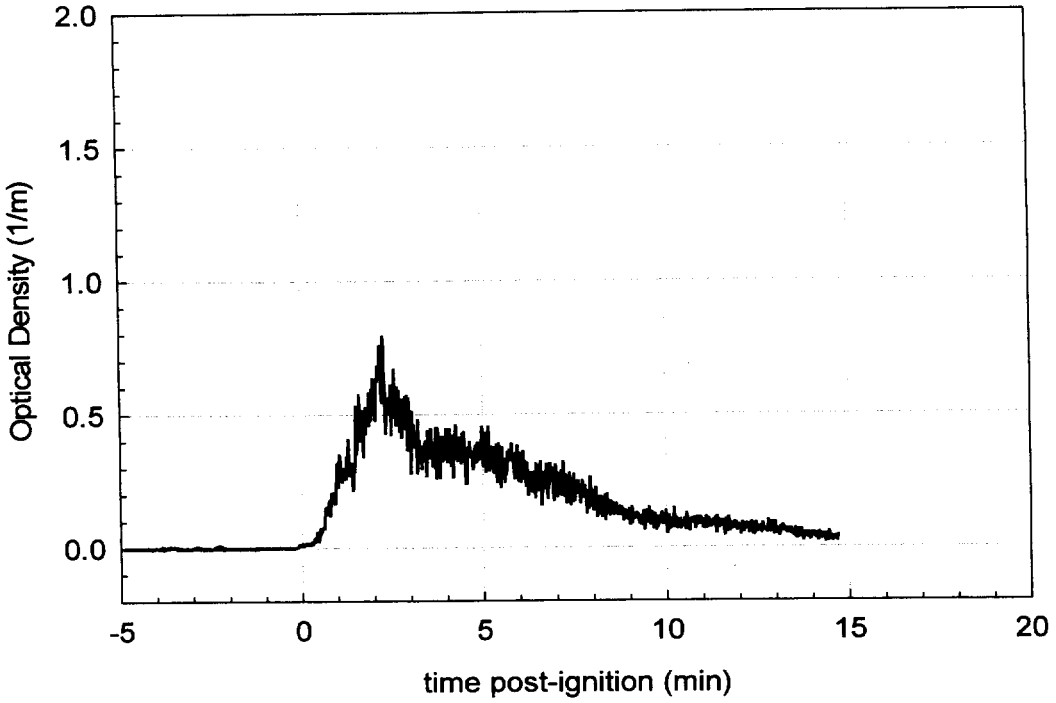

Plot D9. Optical density of air entrained into t he fire products collector at λ = 1.06 μm (infrared) with the FR2 HVAC module.

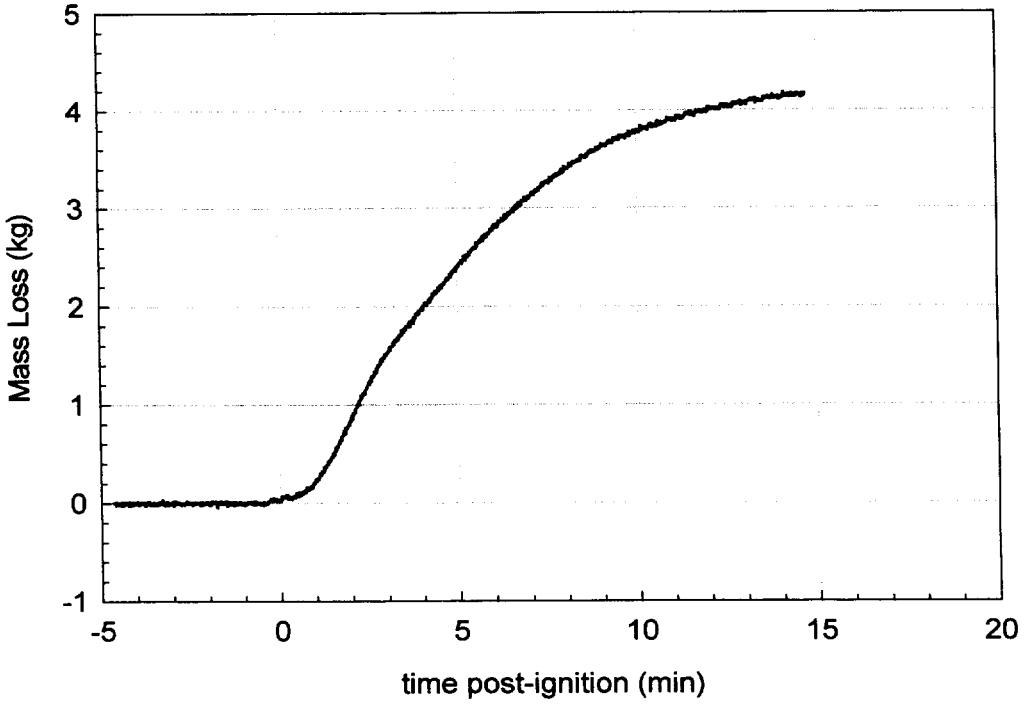

Plot D10. Mass loss from the FR2 HVAC module.